IS-T 1888

Development and Evaluation of High Resolution Quadrupole Mass Analyzer and an Inductively Coupled Plasma-Mach Disk

by

Amad, Ma'an Hazem

PHD Thesis submitted to Iowa State University

Ames Laboratory, U.S. DOE

Iowa State University

Ames, Iowa 50011

Date Transmitted: December 10, 1999

PREPARED FOR THE U.S. DEPARTMENT OF ENERGY

UNDER CONTRACT NO. W-7405-Eng-82.

DISCLAIMER

TABLE OF CONTENTS

LIST OF FIGURES

LIST OF TABLES

CHAPTER 2. A SECONDARY DISCHARGE INTENSIFIES OPTICAL EMISSION FROM A MACH DISK EXTRACTED FROM AN INDUCTIVELY COUPLED PLASMA

CHAPTER 1. GENERAL INTRODUCTION

By definition a plasma is an electrically conducting gaseous mixture containing a significant concentration of cations and electrons. The Inductively Coupled Plasma (ICP) is an electrodeless discharge in a gas at atmospheric pressure. This discharge is an excellent one for vaporizing, atomizing, and ionizing elements. The early development of the ICP began in 1942 by Babat and then by Reed in the early 1960s. This was then followed by the pioneering work of Fassel and coworkers in the late 1960's (1-3). Commercial ICP spectrometers were introduced in the mid 1970s. A major breakthrough in the area of ICP took place in the early 1980s when the ICP was shown to be an excellent ion source for mass spectrometry (4).

Operation of an ICP and the generation of a Mach disk

The plasma is generated and sustained inside the plasma torch. It consists of three concentric quartz tubes through which three flows of argon gas (nebulizer gas flow, outer gas flow, and auxiliary gas flow) pass at a total flow rate of ~16 l/min. These flows sustain the formed plasma and cool the torch. Outside the torch is a water cooled load coil that is powered by a rf generator. The rf generator is operated at either 27 or 40 MHz with a typical rf power of 500-2000 watts. A schematic diagram of the ICP is shown in Figure 1. To generate a plasma, a spark from a Tesla coil produce a seed of electrons. These seed electrons interact with the fluctuating magnetic field to generate a stable plasma.

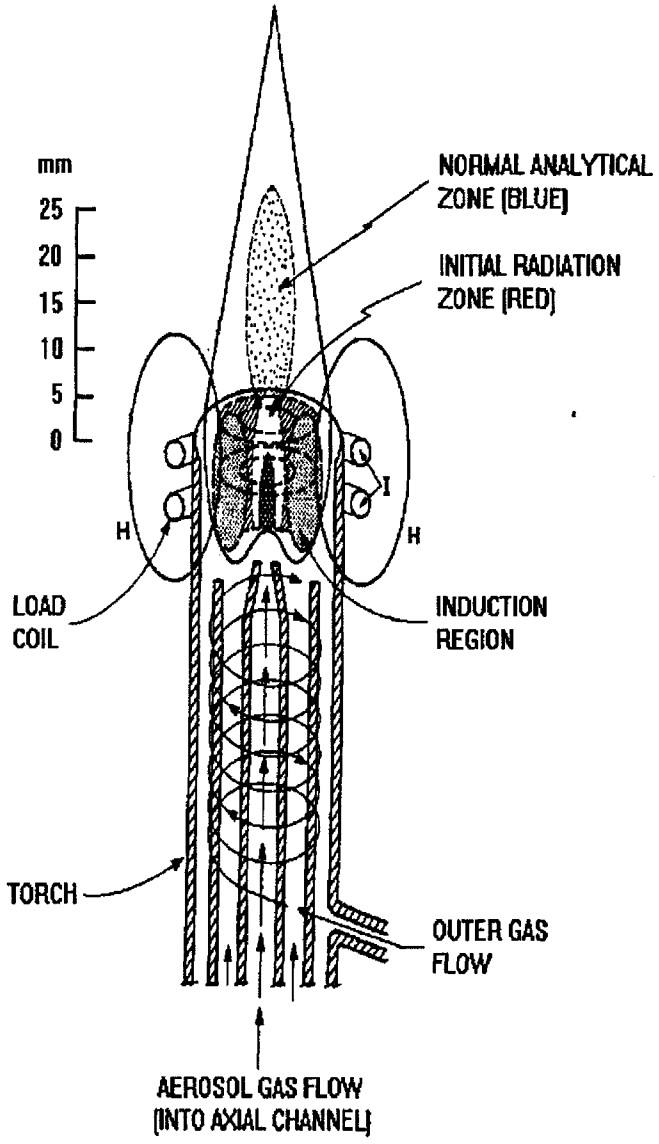

Figure 1. A schematic diagram of the ICP (5).

This stable plasma consists of three distinct bodies: the induction region, the central channel and the plasma tail. The induction region is mainly where energy coupling occurs. As a sample or droplet travels through the central channel, it will undergo desolvation, vaporization, atomization, ionization and excitation. The central channel consists of three zones; the initial radiation zone (IRZ), normal analytical zone (NAZ) and the plasma plume. The NAZ is the plasma region of greatest analytical utility in ICP-MS and ICP-AES.

When an ICP is extracted and sampled through a sampler into a small evacuated chamber by a mechanical pump, a supersonic expansion forms behind the sampling orifice. This expansion consists of a zone of silence, a Mach disk and a barrel shock (Figure 2). The barrel shock and the Mach disk are caused by collisions between fast atoms and ions from the zone of silence and the background gas. The Mach disk is found to be the brightest emission region. Line intensities from the Mach disk were found to be weaker than those obtained from an ICP by a factor of a thousand. However the spectral background was so low that it was indistinguishable from the dark current (6).

The position of the Mack disk is given by

$$X_m/D = 0.67\,[P_0/P_1]^{1/2}$$

where X_m is the distance of the Mach disk from the sampling orifice, D is the diameter of the sampling orifice (1.06 mm), P_0 is the ICP pressure (10^5 Pa, 760 torr) and P_1 is the background pressure in the extraction chamber. In ICP-MS, a 1.0 mm skimmer is placed at a position approximately 2/3 of the offset of the Mach disk location. Gray (7) reported a photographic study of this extraction process.

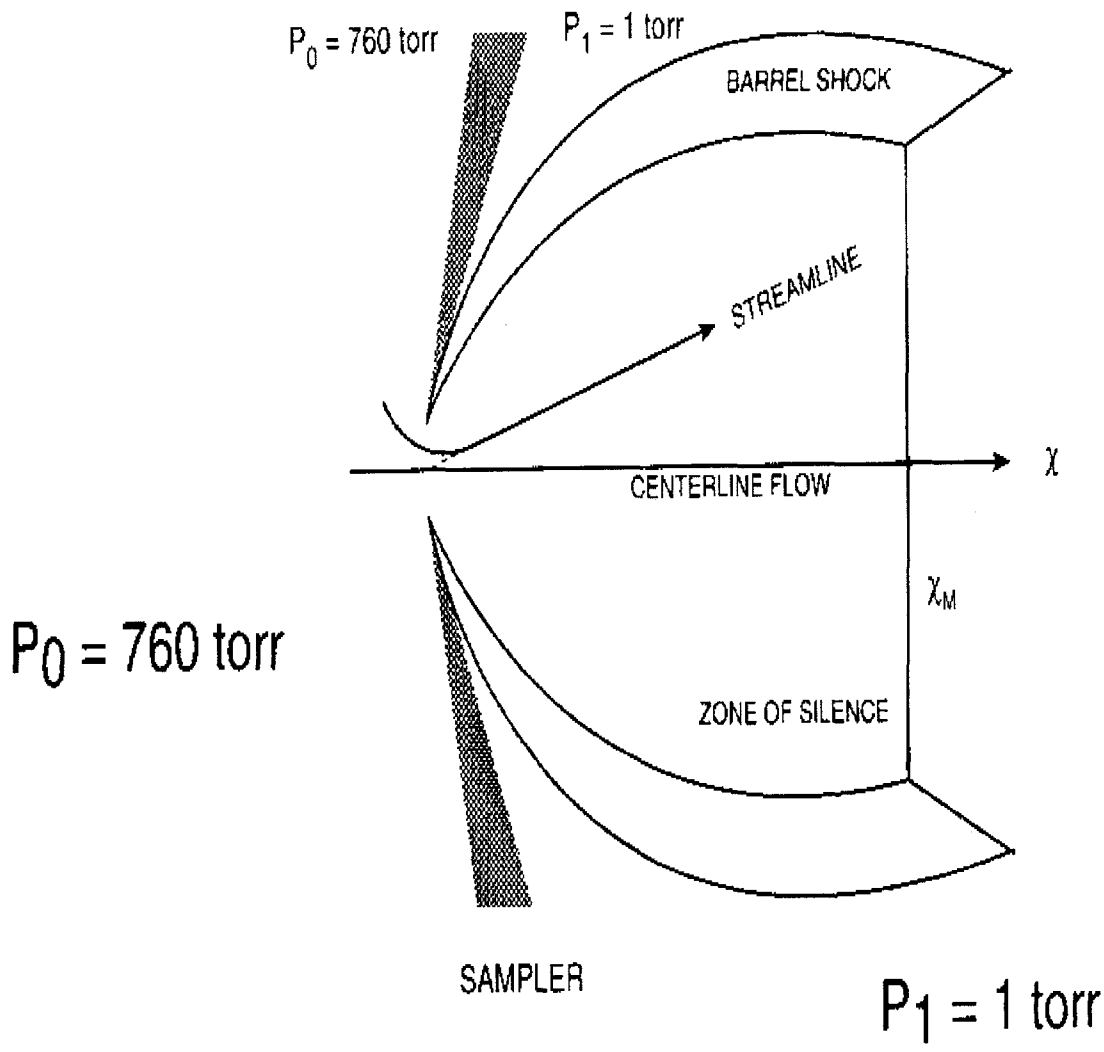

Figure 2. Schematic diagram of the Mach disk and supersonic jet expansion (8).

Secondary Discharge or a Pinch

One of the early initial problems in ICP-MS development was the presence of an electrical discharge formed between the plasma and the sampling orifice (9-14). This secondary discharge or "pinch" is formed due to an rf potential in the plasma. This discharge is strongest at low power, high aerosol gas flow rate, and high water load. The discharge also becomes more intense as the sampler is retracted further downstream in the plasma.

Mass Spectra and Interferences (Low Resolution ICP-MS)

Despite the tremendous capabilities of a quadrupole-based ICP-MS for trace elemental analysis, ICP-MS suffers from the presence of polyatomic ion interferences (15-18). These inferences are most common for ions below m/z 80. A resolution of 5000 at 50 % peak height definition is needed to resolve the major polyatomic ion interferences in ICP-MS. When pure water is nebulized into the central channel of the plasma, Ar, O, H, and N atoms are the most important elements in the plasma. Some of these atoms are ionized, so that Ar^+, O^+, H^+ and N^+ ions are found in the background spectrum.

In addition, some polyatomic ions are found in the background spectrum such as OH^+, H_2O^+, H_3O^+, O_2^+, ArH^+, ArO^+ and Ar_2^+. Usually the sample is not dissolved in pure water but in an acid solution. In this case additional polyatomic ions are formed and are detected in the blank.

Most systems for ICP-MS are based on quadrupole mass analyzers operated at unit mass resolution in the first stability region. These systems usually cannot separate chemically different ions at the same nominal m/z value. A high resolution device such as a

magnetic sector or Fourier transform – ion cyclotron resonance instrument can resolve such pairs of interfering ions and can determine the elemental formula of an organic compound from accurate measurements of the m/z value of the parent ion. High-resolution selection of the parent ion in the first stage of a tandem MS also greatly improves the selectivity of a particular parent ion – daughter ion channel in collision induced dissociation for analysis of complex mixtures. If the resolution of a quadrupole could be improved, then such measurements would be possible without the additional size, complexity and expense associated with the usual type of high-resolution mass analyzer.

Mass Analyzers

Mass spectrometry is the most comprehensive and versatile of all instrumental methods of analysis. Almost any material can be analyzed with a suitable mass spectrometer. Every mass spectrometer, regardless of its design is comprised of three functional elements: (1) the source, where ions that represent the sample are generated; (2) the analyzer, where the separation of ions occurs in space or time; (3) the detector, where ions of interest are detected.

Most mass spectrometers are used to answer the basic question of what is present and how much is present in a particular sample by determining ionic masses and abundances. The most important characteristics of a mass analyzer are the instrumental resolution and sensitivity. The resolving power or resolution of a mass spectrometer is a measure of its ability to separate, resolve and identify ions of slightly different masses. Sensitivity is dependent upon the detector and upon the ionization technique used. The sensitivity of a

mass spectrometer is a measure of the instrument response to ions of a particular component at a given m/z value.

In practice, resolution can be determined using an isolated peak in the mass spectrum. Resolution, R, can be simply determined from the formula $R = m/\Delta m$, where m is the mass of the peak in atomic mass units and Δm is the peak width at some specified fraction of the peak height (often 50 % or 10 %). The 5% peak width definition is technically equivalent to the 10 % valley definition. The valley definition is the most popular term, which expresses resolution in terms of the highest mass at which two adjacent peaks of equal height exhibit a valley between the peaks not greater than a certain percentage of the peak height.

Sensitivity and resolution are usually inversely proportional to each other. In most applications there is a trade off. In a magnetic sector, the trade off is accomplished by adjusting the slit widths. Figure 3 shows the trade off between sensitivity and resolution.

The first mass spectrometer was introduced by Thomson in 1910 (19) and later by Aston in 1919 (20). Aston introduced the concept of velocity focusing to provide information about isotopes and atomic structure. Dempster developed the 180^0 deflecting magnetic sector (21-23). Mass spectrometers with different geometry (90^0 and 60^0) were introduced by Nier (24,25). These devices were known as static analyzers.

There are four general advantages of high-resolution capability in mass spectrometry:

1. To separate analyte ions from interfering ions at the same nominal m/z value, e.g, to separate $^{12}C^{16}O^+$ (m/z = 27.99437) from $^{14}N_2^+$ (m/z = 28.0056) and thus analyze a mixture of CO and N_2.

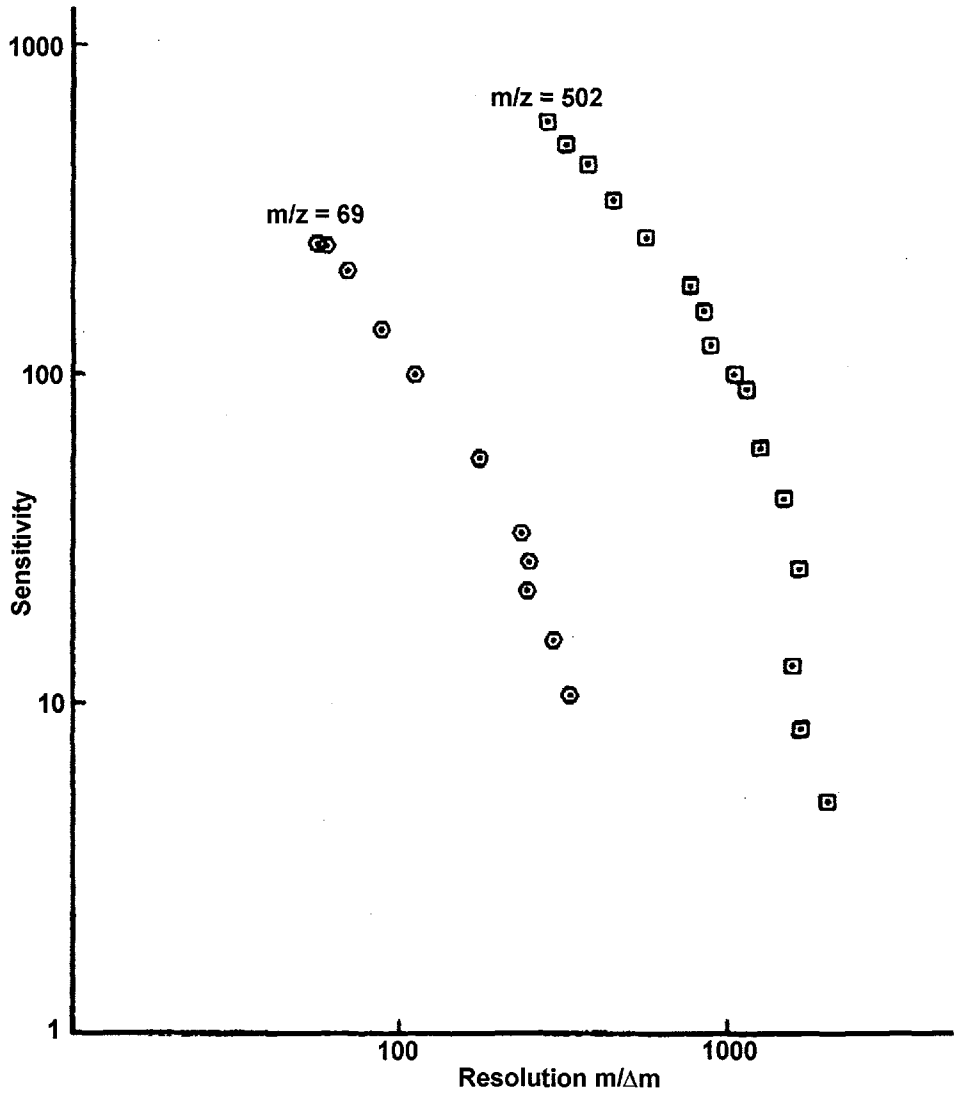

Figure 3. The trade off between sensitivity and resolution (26).

2. To identify the elemental formula of organic ions by accurate measurement of the m/z value of the parent ion.
3. To resolve the isotopic structure and help identify the formula of large, multiply charged ions produced by electospray MS.
4. To provide more selective isolation of a parent ion to be fragmented subsequently to provide structural information in a tandem MS measurement.

The quadrupole mass filter is by far the most common type of mass spectrometer. It has proven to be rugged and reliable. Resolution and peak shapes are affected by the mechanical accuracy with which the rods are constructed and mounted (26). In a given quadrupole, the resolution is proportional to the square of the number of RF cycles the ions spend inside the rods (27). Thus the resolution can be improved greatly by allowing the ions to stay inside the rods for more cycles. The obvious ways to keep ions inside the rods longer and the associated problems are as follows:

1. Increase the length of the rods (L) – This was investigated by von Zahn (28), who constructed a rod set that was 5.8 m long and was designed to provide a resolution of 16,000. In general, however, increasing L makes the rods larger and heavier, which defeats the advantages of small size. Long rods require more electrical power; they are also much more difficult to construct and mount with the required dimensional tolerance (±10 μm or better).
2. Increase frequency (f) – For a given rod diameter, the maximum m/z value that can be transmitted decreases as f increases, so increasing frequency compromises mass range. In applications such as ICP-MS, where atomic ions are used and mass range is not much

of an issue, improvements in abundance sensitivity have been reported by increasing the RF frequency.

3. Inject ions with low kinetic energy (V_z) – Slow ions are injected less efficiently and stay longer in the fringe fields at the entrance and exit of the mass analyzer. Even the analyte ions that are stable inside the rods are deflected by the weak DC and RF potentials in the fringe fields, which compromises transmission and causes mass discrimination

Geometry and Principle of Operation of a Quadrupole Mass Analyzer

The quadrupole mass analyzer employs a combination of direct current (DC) and radio-frequency (RF) potentials as a mass filter (29). The general layout of the quadrupole mass filter is shown in figure 4. It consists of four parallel rods arranged symmetrically. In an ideal arrangement, these four rods should have the shape of hyperbola; however in practice, cylindrical rods are often used. Opposing rods are connected together electrically to the DC and RF voltages. Ions are extracted from the source into the quadrupole region between the four rods and along the longitudinal axis. As ions wobble inside the rods they are influenced by the combined DC and oscillating rf field. As ions drift inside the poles along the z axis, their motion in the x-y plane can be expressed in terms of the Mathieu equation, which define a and q parameters as follows:

$$a_x = -a_y = 4eU/m\omega^2 r_o^2$$

and

$$q_x = -q_y = 2eV/m\omega^2 r_o^2$$

where a is the parameter in the Mathieu equations of motion which depends upon U, U is the

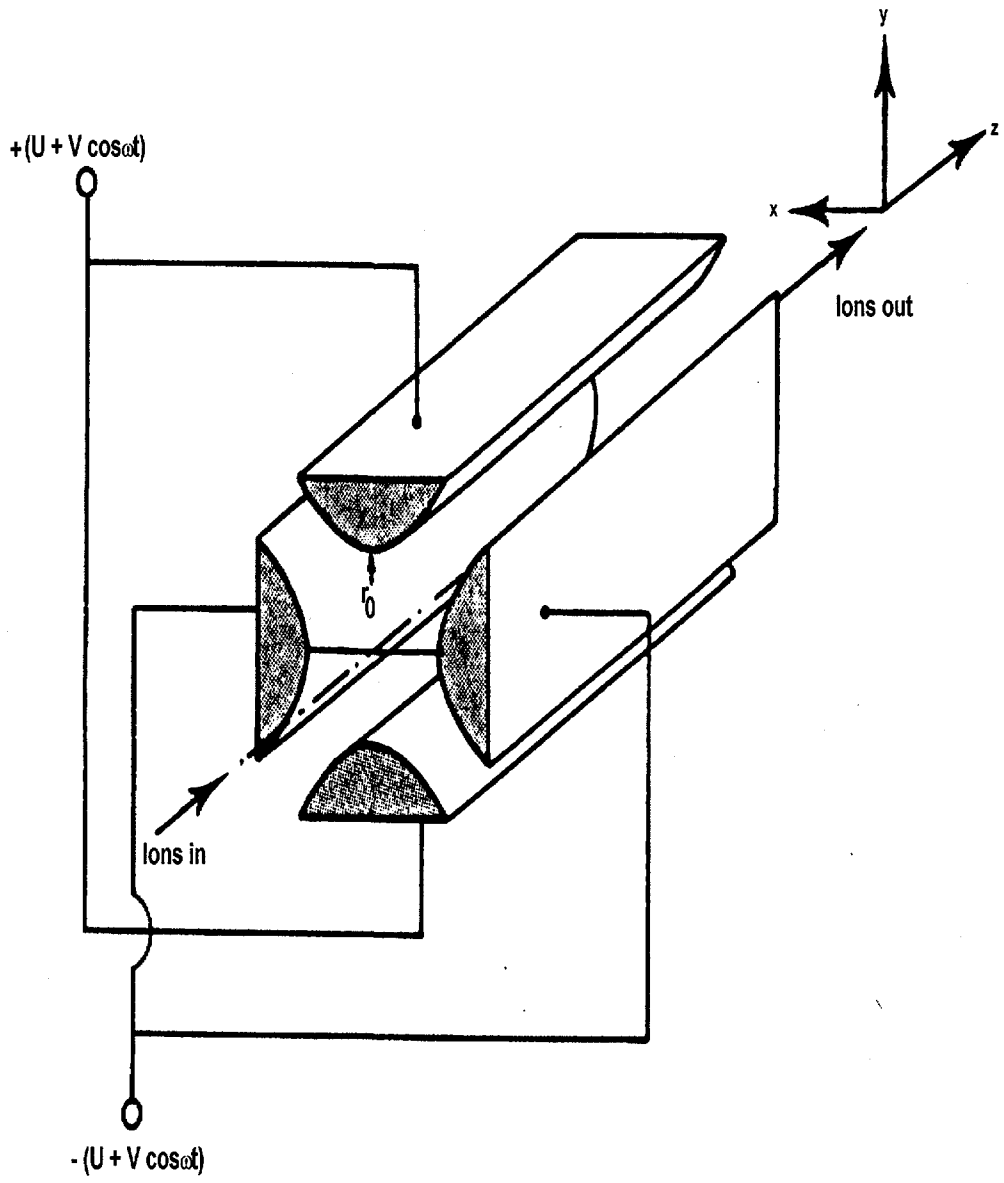

Figure 4. Schematic diagram of a quadrupole mass filter (26).

d.c. voltage applied between opposite sets of electrodes, q is the parameter in the equations of motion which depends upon V, V is the zero-to-peak rf voltage applied between opposite sets of electrodes, e is the electronic charge, m is the ionic mass, ω is the angular frequency of the applied field ($\omega = 2\pi f$ where f is in Hertz) and r_o is the field radius inscribed inside rods. The equations of ion motion are given by $mx = eE_x$ and so on. That is

$$d^2x/dt^2 = x^{\cdot\cdot} + (e/mr_o^2)\,\phi_o\, x = 0 \ldots\ldots\ldots\ldots(1)$$

$$d^2y/dt^2 = y^{\cdot\cdot} + (e/mr_o^2)\,\phi_o\, y = 0\ldots\ldots\ldots\ldots(2)$$

$$d^2z/dt^2 = mz^{\cdot\cdot} = 0\ldots\ldots\ldots\ldots\ldots\ldots\ldots\ldots(3)$$

where E_x is the ion energy in the x axis direction, and ϕ_o is the potential applied between opposite sets of electrodes. Equation, 1 and 2 give the ion motion in the xz and yz planes when ions are injected ions into the quadrupole mass analyzer with a given velocity in the z direction. If the potential ϕ_o is constant, there will be a simple harmonic motion in the xz plane for any ion injected into the quadrupole and all ion trajectories would be stable. This condition for ion stability is expressed and explained in what is known by the stability diagram. The parameters a and q define the stability diagram. The diagram shows regions of (a ,q) in which ions have a stable or unstable ion trajectory in the quadrupole field. The stable ion trajectories describe the paths of ions passing through the analyzer without touching the rods (figure 5). The unstable ion trajectories describe the paths of ions that hit the quadrupole rods and are therefore lost from the system. A whole series of stability regions exists from

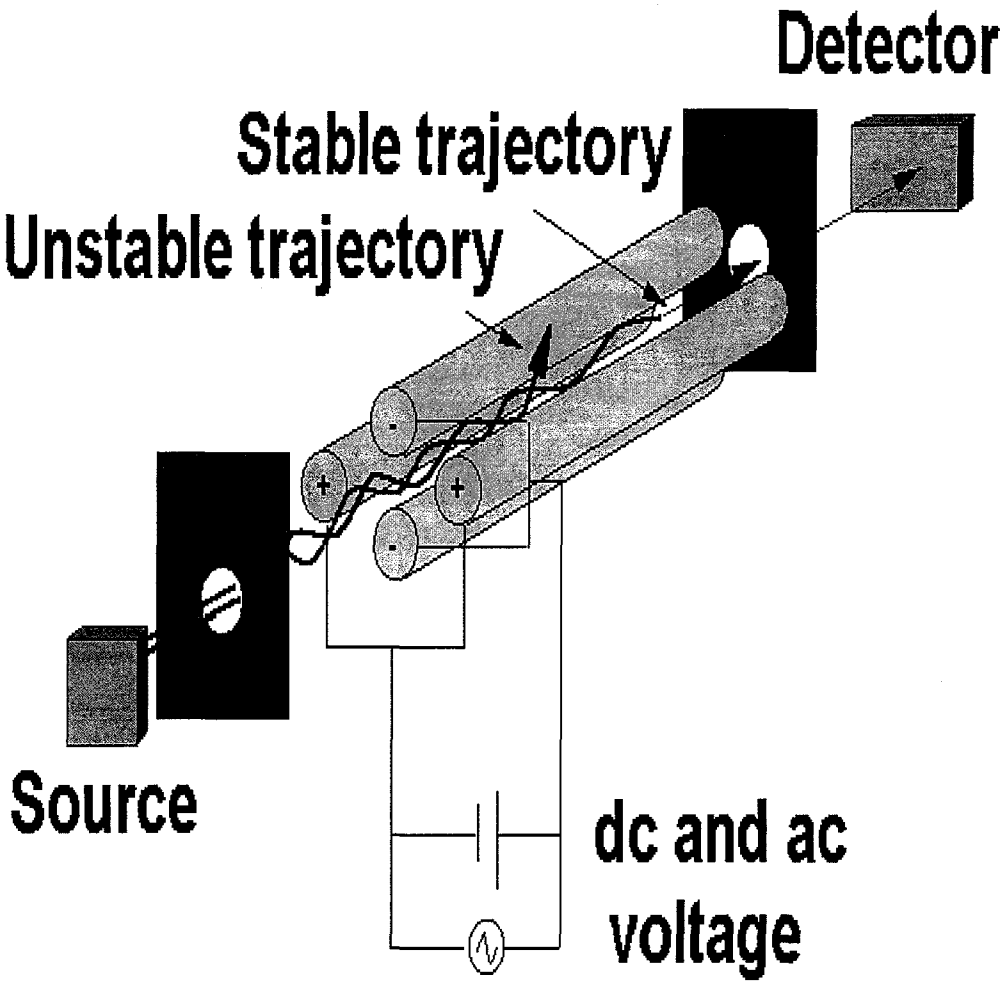

Figure 5. The stable trajectory in a quadrupole (30).

the solution of the Mathieu equation. Most commercial systems operate at the first stability region (Figure 6).

An important note is that a line representing the ratio a/q = 2U/V can be drawn on the stability diagram (see figure 7). In this line, the ratio of a/q is held constant while the absolute values of a (U) and q (V) are increased. Such a line is known as a mass scan line and passes through the origin through regions of x stability and y instability before crossing into the area of both x and y stability.

The quadrupole mass spectrometer is capable of scanning the mass spectrum in a few milliseconds. Its advantage compared with magnetic sector instrument is that the resolution of the analyzer can be adjusted electronically by adjusting the U/V ratio and that there is a linear relation between the number and the magnitude of the applied voltages U or V.

Resolution, Mass Range and Abundance Sensitivity

There are three important operating characteristics of quadrupole, the maximum mass range, the resolution and the abundance sensitivity. The resolution and the mass range depend on five basic factors. These factors are the length of the rods, the diameter of the rods, the supply voltage on the rods, the rf frequency and the injected ion energy.

The maximum mass is given by the following relation

$M_m = 7 \times 10^6 V_m / f^2 r_o^2$

where V_m is the rf voltage applied between adjacent rods, r_o is the inscribed radius of the rods (m) and M_m is the maximum mass measured in Da.

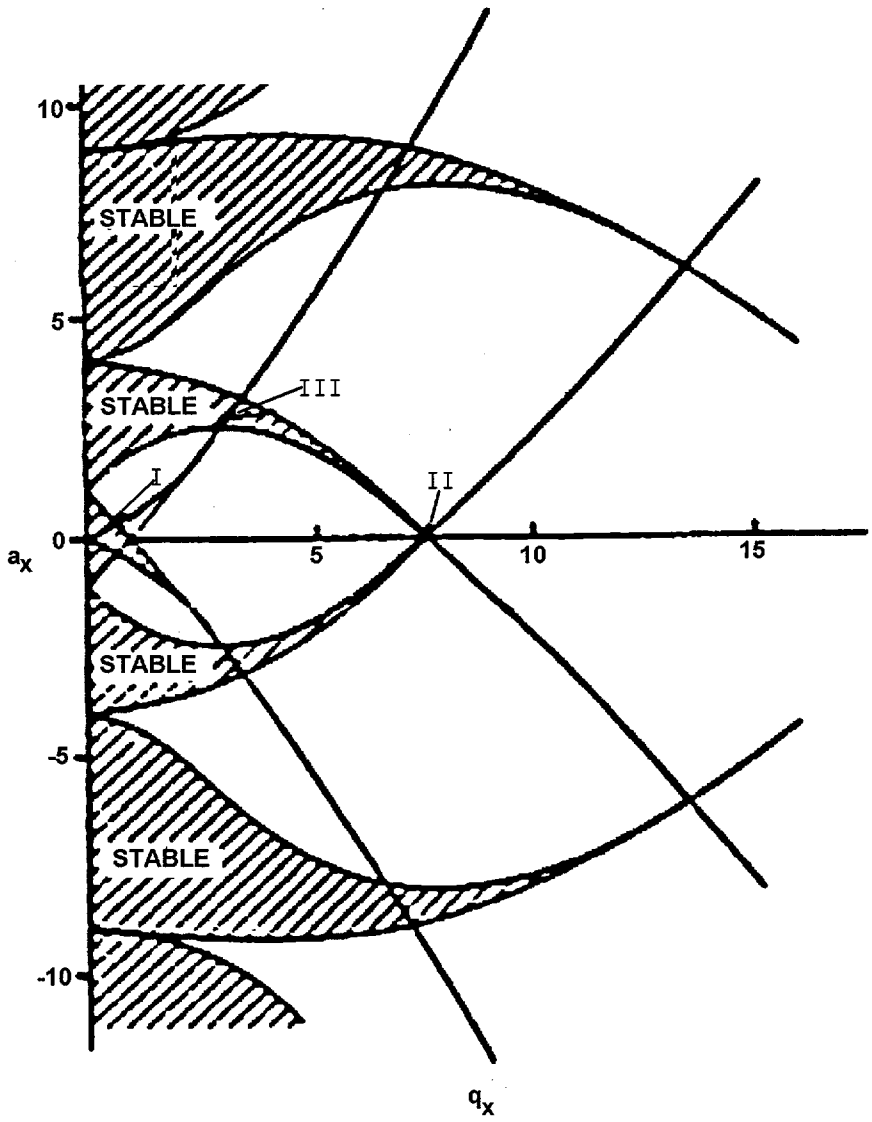

Figure 6. The stability diagram (26).

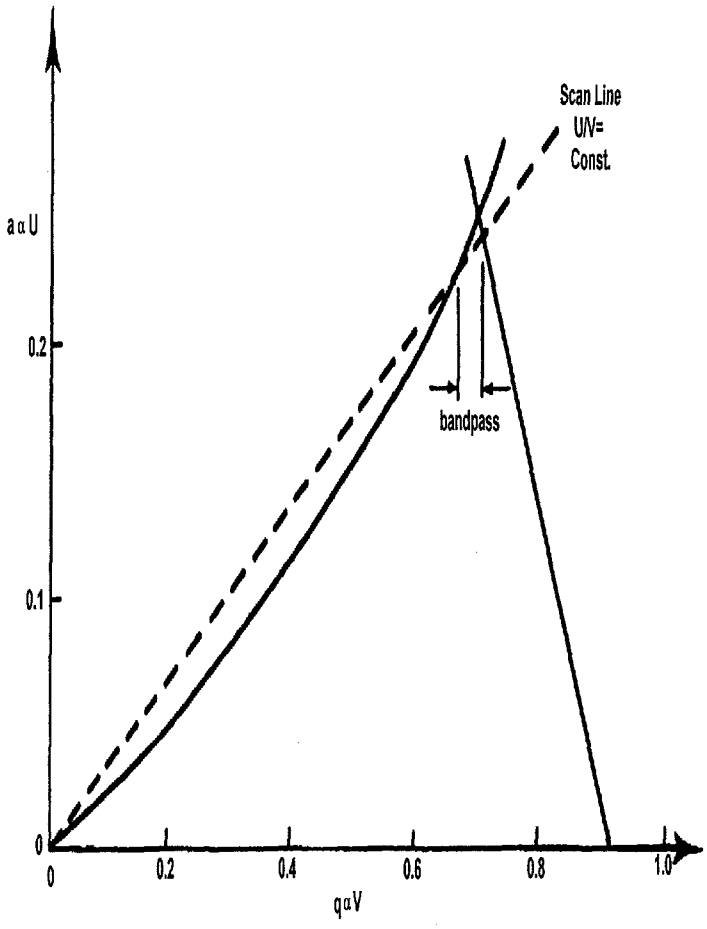

Figure 7. The mass scan line.

The resolution of a given quadrupole mass analyzer is limited by the selection of a mass range. The finite analyzer length imposes one limitation on the resolution. The finite length of the quadrupole rods limits the time spent by an ion in a stable trajectory and hence limiting the resolution. It is well established that the resolution of a quadrupole is limited by the number of rf cycles the ion spends inside the rods.

For a given quadrupole, the resolution R should be roughly proportional to the square of the number of RF cycles n the ions spend inside the rods:

$$m/\Delta m = R = n^2/K = \quad \propto \quad m f^2 L^2/ zV_z$$

where m = m/z value of the ion measured and Δm = peak width at some specified fraction of the peak height (often 50% or 10%) (see figure 8), R is the resolution, n is the number of cycles, K is an empirical constant, m is the ionic mass, V_z the ion injection energy, f is the rf frequency and L is the length of the quadrupole. Figure 9 shows the dependence of maximum resolution on the number of rf cycles.

As an example of the calculation of resolving power, let us consider what resolving power is needed to separate ions $^{56}Fe^+$ and $^{40}Ar^{16}O^+$. Since resolving power is defined as mass to be measured divided by the difference in mass to be separated ($m/\Delta m$), a resolution of

$$56/0.022355 = 2502$$

is thus required.

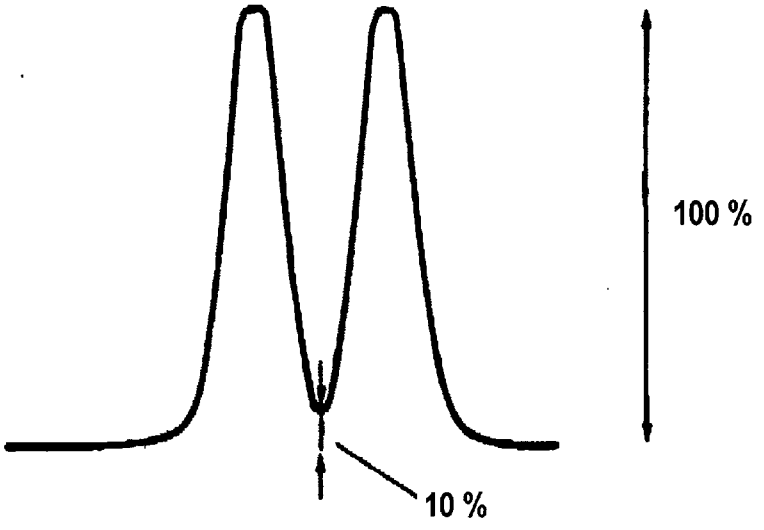

Figure 8. Representation of the 10 % valley definition of resolution.

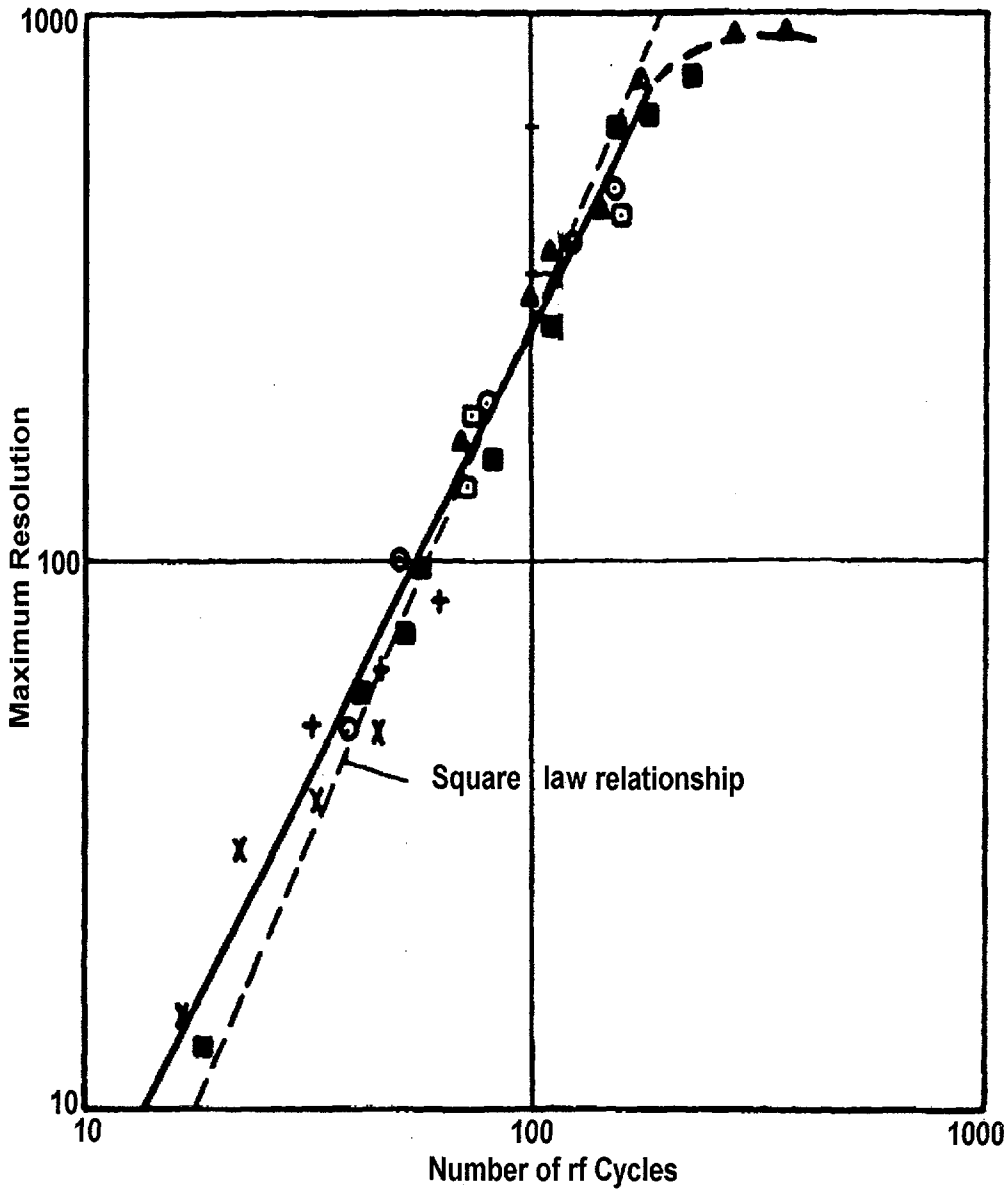

Figure 9. Dependence of resolution on n (26).

The abundance sensitivity (AS) is another performance characteristic of a mass analyzer. It gives a measure of the extent to which the tails of the peak at mass m contribute to peaks at masses (m-1) and (m+1), and can refer to peak area as well as to peak height. When peak area is considered the integrated width must be specified. With reference to figure 10, the abundance sensitivity is given by:

AS (low mass, height) = h_{m-1}/h_m

AS (low mass, area) = a_{m-1}/a_m

AS (high mass, height) = h_{m+1}/h_m

AS (high mass, area) = a_{m+1}/a_m

High Resolution Quadrupole Mass Spectrometry in Alternative Stability Regions

Quadrupole mass filters are normally operated in the first stability region. These filters are considered to be low-resolution devices operating at a unit mass resolution (26,31). Higher resolution can be obtained with a quadrupole mass analyzer if it is operated at higher regions (32-34). However with the successful development of commercial instruments commonly using the region labeled by I, the higher stability zones have been ignored and neglected for reasons listed below:

1. The necessity of using higher operating voltages than that of a conventional filter operated at a first stability region.
2. The upper level of the mass filter passing band.
3. The necessity of using a prefilter to eliminate ions with $q < 0.908$ for region II.

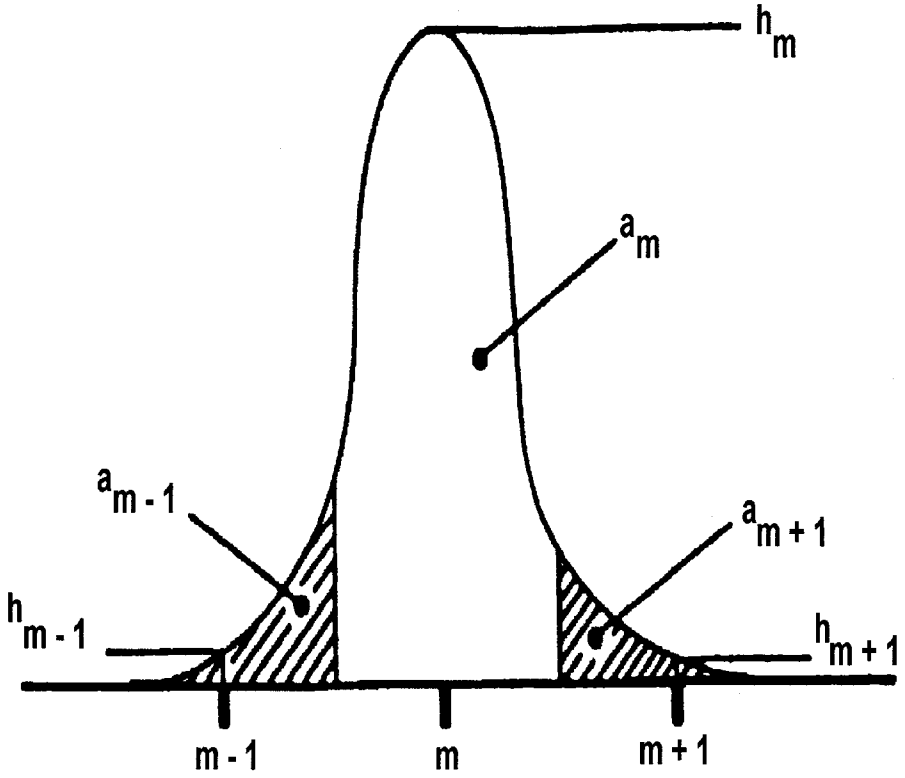

Figure 10. Abundance sensitivity.

4. The presence of higher fringing fields.

Figure 6 shows the regions where ion motion is stable in the x and y direction which is expressed in terms a and q. The well-known region I, near the origin, is used in normal mass filters.

Second stability region

The quadrupole mass analyzer can be operated at a stability region near a = 0, q = 7.547. This region is known as the II stability zone (35). This region was suggested by Post and is shown in figure 11. If the quadrupole is operated in an rf mode (a=0) the width of the base line corresponds to a resolution of 114. Dawson and Binqi (36,37) showed resolution of $^{131}Xe^+$ from $C_3F_5^+$ ($m/\Delta m$ =1500) with an ion energy of 300 eV. Hiroki and coworkers (38) obtained a unit mass resolution on 3.0 keV ions of N_2^+ and O_2^+.

In contrast to normal operation (zone I), low energy ions (e.g. 20 eV) cannot be effectively injected into the quadrupole because of the fringe field effect. In the second region the fringe fields are strongly defocusing. The overall sensitivity was about an order of magnitude less than that obtained in the normal region but the source and ion optics should be modified to inject ions with high kinetic energy.

Douglas and Ying (39) have investigated the second region for ICP-MS. A resolution (R) of 5000 at m/z 56 was demonstrated. At this resolution $^{40}Ar^{16}O^+$ from $^{56}Fe^+$ were sufficiently resolved. One potential advantage of using high energy ions in a quadrupole mass analyzer is that the analyzer can be scanned fast.

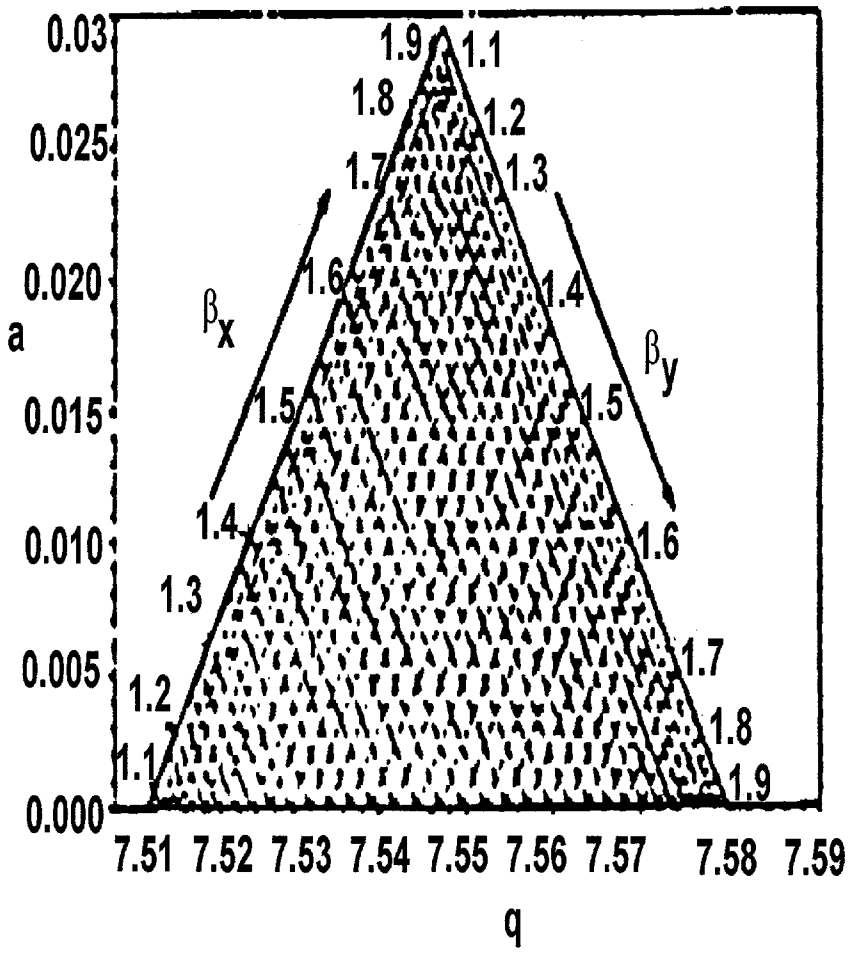

Figure 11. Second stability region (35).

Third stability region

The third stability region has a rectangular shape in which a resolution can be obtained in two sharp regions (40). The upper one is labeled M (41,42) and the lower one is labeled K (43). Figure 12 shows the operation areas of these zones near the two sharp tips.

Konenkov et al. (44) operated a quadrupole at the upper tip of region III to separate CO^+ and N_2^+ ions (m/Δm 2500), $^{20}Ne^+$ and D_2O^+ (m/Δm 656) and He^+ from D_2^+ (m/Δm = 157)(38). Douglas and coworkers (45) used the M tip to resolve ArO^+ from Fe^+ from ions extracted from an ICP. An advantage of the third stability region is the ability to analyze ions of high energy 10-100 eV. Again, the fringing fields of the third stability region are more strongly defocusing than those of the first stability region. A quadrupole with mediocre mechanical precision can still give a good peak shape operated at high resolution. Therefore the peak shape is better than in region one.

Other stability region

There are many other stability regions in the stability diagram that are not well studied. One such region is near a = 0 and q = 21.3. This region is very similar to the second region and it is a small triangle shape (46). Another region is near a =7 and q=7. In this region Konenkov (47) reported the first spectrum. In all these unexplored regions a higher resolution and the ability to analyze ions with higher kinetic energy can be obtained.

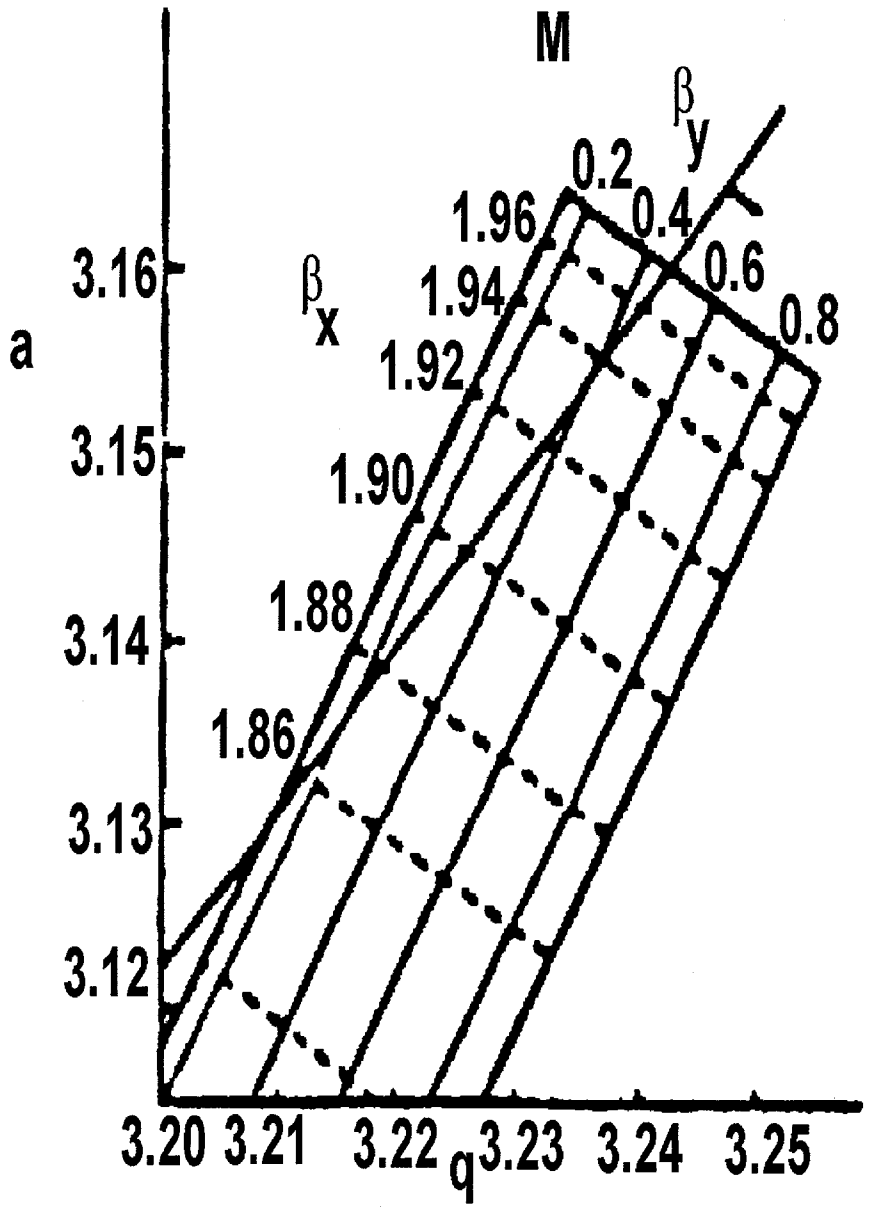

Figure 12. Third stability region (40).

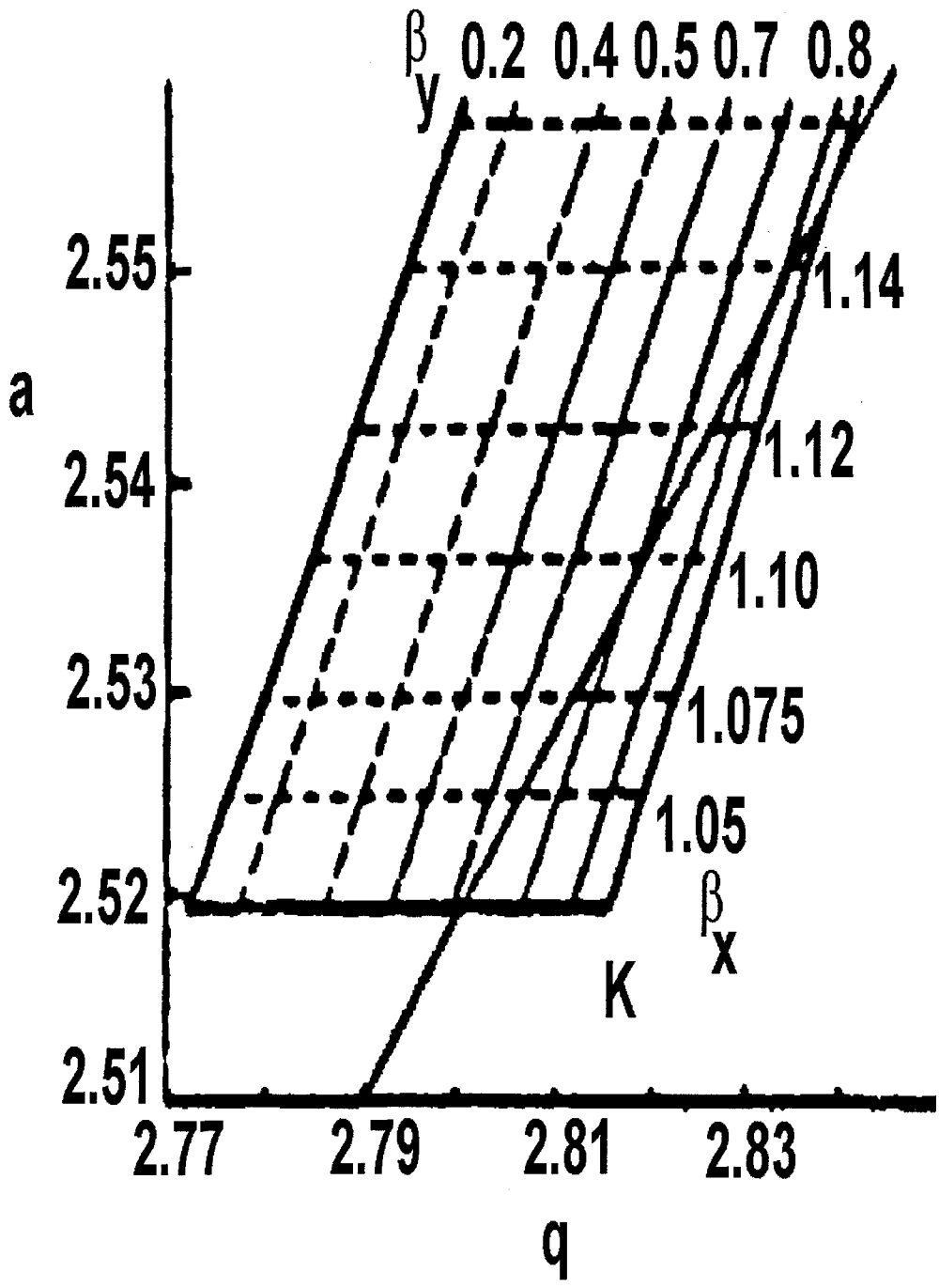

Figure 12. Cont.

Over Resolving Modulaters

Another way to improve resolution is described by de Maack, Devant and Rolando (48). These workers achieve resolution of 10,000 using "a periodically over-resolving modulation," which amounts to an additional RF potential of lower frequency and amplitude applied to the rods. The additional RF component moves the working point slightly closer to the tip of the stability diagram which improves the resolution.

Dissertation Objective and Organization

This dissertation is presented as three chapters, each of which stands alone as a complete scientific manuscript with accompanying references, tables and figures. Each chapter is a paper either published in or submitted to a research journal. A general conclusions section, summarizing the significant results of this thesis, is presented in the final chapter.

Chapter 2 of this thesis aims at the detection limits for simultaneous multielement analysis by ICP-AES techniques. With the new development of the SCD-based ICP optical spectrometers, the detection limits were shown to be only limited by the photon shot noise of the ICP spectral background. One possible way to improve the detection limits is to reduce the spectral background. It has been demonstrated that the spectral background emitted from the reduced pressure plasma extracted from an ICP is very low and can not be distinguished from the dark current of the photomultiplier used. In addition it has been shown that the analyte line intensities from the Mach dish are low. To enhance the line intensity from the Mach disk while keeping the spectral background low we employed a mild discharge between the plasma and the

sampling orifice. In this chapter we demonstrated that a mild discharge does improve the detection limits of an ICP-MD-AES by a bit in a simultaneous multielement mode but more work is needed to improve its capability to match the superior detection limits obtained in ICP-MS.

Chapters 3 and 4 of this dissertation aim to improve the resolution of a quadrupole mass filter by reflecting the ions several passes inside the rods of the analyzer. In particular, the resolution should increase with n^2, so there should be substantial room for improving resolution if the number of RF cycles n can be increased significantly. The present work presents initial results that suggest that resolution can be improved by simply reflecting ions back and forth through a quadrupole operated in the usual stability region. Even only three passes would increase L and n by a factor of three, so resolution should improve by a factor of $3^2 = 9$. Techniques for reflecting ions are highly developed with the reflectrons used in time-of-flight MS. In addition chapter 4 incorporates a gated electron impact ion source. In this arrangement finite, non-continuous batches of ions are reflected in the quadrupole and the ion source will function as a storage device. Chapter 5 provides future work and a general conclusion.

References

1. Wendt, R.H and Fassel, V.A., *Anal. Chem.*, 1965,**37**,920.
2. Fassel, V.A. and Kniseley,K.N., *Anal. Chem.* 1974, **46**, 1110 A and 1115A.
3. Greenfield, S., Jones, J.L. and Berry, C.T., *Analyst*, 1964,**89**, 713.

4. Houk, R.S., Fassel, V.A., Flesch, G.D., Svec, H.J., Gray,A.L. and Taylor, C.E., *Anal.Chem.*, 1980,**52**,2283.

5. Fassel,V.A, Pure *Appl. Chem.*,1977,**49**,1533.

6. Houk,R.S., and Lim, H.B., *Anal. Chem.*, 1986,**58**,3244.

7. Gray, A.L., *J.Anal.Atomic Spectrom.*, 1989,**4**, 365.

8. Hongsen, N. and Houk,R.S. Spectrochemiacta, Part B, 1996, 51, 779.

9. Gray, A. L., Houk, R. S., and Williams, J. G., *J. Anal . Atomic Spectrom.*, 1987, **2**, 13.

10. Olivares, J. A., and Houk, R. S., *Appl . Spectrosc.*, 1985, **39**, 1070.

11. Lim, H. B., Carney, K. P., Edelson, M. C., Houk, R. S., and Brenner, I. B.,*SpectrochimActa, Part B*, 1993, **48**, 1617.

12. Houk, R. S., LaFreniere, B. R., Lim, H. B., and Fassel, V. A., *Appl . Spectrosc.*, 1987, **41**, 391.

13. Tan, H., Ishii, I., and Montaser, A., *J . Anal . Atomic Spectrom.*, 1991, **6**, 317.

14. Gray, A.L, and Williams, J.G., Z ., *J. Anal. Atom, Spectrom.*, 1987, **2**, 599.

15. Horlick, G., Tan, S.H. Vaughan,M.A., and Rose, C.A., *Spectrochim. Acta* , 1985, **40B**, 1555.

16. Horlick, G., Tan, S.H. Vaughan,M.A and Shao, Y. *Analytical Atomic Spectrometry*, eds. Montaser, A, and Golightly, D.W., VCH Publishers, New York, pp.361-398.

17. Jarvis, K. E., Gray, A. L., and Houk, R.S., *Handbook of Inductively Coupled Plasma Mass Spectrometry*, Blackie & Son, Glasgow, 1992.

18. Houk, R.S., *Anal. Chem.*,1986, **58**, 97A-105A.

19. Thomson, J.J., *Rays of positive electicity and their application to chemical analysis*, Green and Co., London, 1913.

20. Aston, F.W., *Mass Spectra and Isotopes*, Arnold, London, 1942.

21. Dempster, A. J., *Phys. Rev.*, 1918,**11**,316.

22. Dempster, A J., *Phys. Rev.*, 1921,**18**,415.

23. Dempster, A. J., *Phys. Rev.*, 1922,**20**,631.

24. Nier, A.O. *Rev. Sci. Instr.* 1940, **11**,212.

25. Nier, A.O. *Rev. Sci. Instr.* 1947, **18**,398.

26. Dawson, P. H., Ed. *Quadrupole Mass Spectrometry and Its Applications*, Elsevier,Amsterdam, 1976.

27. Titov, V.V. *J. Amer. Soc. Mass. Spectrom.* 1998,**9**, 50,70.

28. von Zahn, *U. Z. Phys.* 1962, **168**, 129-142.

29. Paul, W.,and Steinwedel., H., *Z. Naturforsch.* 1953, **8a**, 448.

30. Wesdemiotis,C.,*http://www.chemistry.uakron.edu/www-research/cw-ewb/boss.html.*

31. Slobodenuk, *Quadrupole mass Spectroneters*, Atomisdat, Mosco, 1974.

32. Dawson, P.H.; Binggi, Y., *Int. J. mass. Spectrom. Ion processes*, 1984,**56**,25.

33. Dawson, P.H.; Binggi, Y., *Int. J. mass. Spectrom. Ion processes*, 1984,**56**,45.

34. Post. R.F, Univ. Cal. Radiat.Lab.Rwp.U.C.R.L. 1953,2209.

35. Kalashnikov, M.V., Konenkov, N.V., Shagimuvatov, G.I and Kratenko, V.I.. *Sov. J.Tech. Phis*, 1989,**1**,170.

36. Dawson, P.H., Binqi, Y. *Int. J. Mass Spectrom. Ion processes*. 1984, **56**,25.

37. Dawson, P.H., Binqi, Y. *Int. J. Mass Spectrom. Ion processes*. 1984, **56**,41.

38. Hiroki. S, Abe,T. , Murakami, Y. *Rev. Sci. Inst.*, 1992,**63**,3874.

39. Ying, J.F, and Douglas, D.J. *Rapid Commun. Mass spectrom.* 1996,**10**,649.

40. Shagimuratov, G.I, Konenkov, N.V.; Silakov, S.S.; and Mogichenko,G.A, *Sov. J. Tech.Phys*, 1990, **1**, 112.

41. Konenkov, N.V, Mogilchenko, G.A, Silakov, S.S and Shagimuratov, G.I., *Sov.J.Tech.Phys*. 1990,**1**,117

42. Konenkov, N.V, Mogilchenko, G.A, Silakov, S.S and Shagimuratov, G.I., *Sov. J. Tech. Phys.* 1990,**10**,148.

43. Konenkov, N.V., Mogilehenko,G.A and Silakov, S.S.. *Sov. J. Tech. Phys*. 1990, **6**, 128.

44. Konenkov, N.V., Mogilchenko, G.A., Sikakov, S.S. and Shagimuratov, G.I., *Prib. Tekb. Eksp.*, 1990,**2**,179.

45. Du, Z.D, Olney, T.N. and Douglas, D.J. *J. Am. Soc. Mass Spectrom.* 1997, **8**, 1230.

46. Konenkov, N.V. and Kratenko, V.I. *Int. J. Mass Spectrom. Ion. Processes*,1991,**108**,115.

47. Konenkov, N.V., *Elektronic Tekh: Ser: Electrovakh Gasocydel.* Apparal.,1991,**3**,14.

48. de Maack, F.; Devant, G.; Lapetit, G.; Rolando, C. 36th ASMS Conf. On Mass Spectrom. Allied Topics, San Francisco, CA, Paper No. 817.

CHAPTER 2. A SECONDARY DISCHARGE INTENSIFIES OPTICAL EMISSION FROM A MACH DISK EXTRACTED FROM AN INDUCTIVELY COUPLED PLASMA

A paper published in the Journal of Analytical Atomic Spectrometry[1]

Ma'an H. Amad and R. S. Houk[2]

Abstract

The axial channel of a conventional argon inductively coupled plasma (ICP) is extracted through a circular orifice into an evacuated quartz chamber. Emission from the Mach disk region is focused on the entrance slit of an echelle spectrometer equipped with two segmented-array charge-coupled-device detectors (CCDs). The background pressure in the extraction chamber is 1000 Pa (7.5 torr). At this pressure two barrel shocks and Mach disks are visible. Deliberate use of a mild secondary discharge between the plasma and the sampler enhances emission from the Mach disk for a variety of lines from typical analytes (Ca, Sr, Mg and Mn) by factors of 11 to 25. Detection limits are in the range 0.1-2 $\mu g\ l^{-1}$. Sodium chloride at concentrations up to 10,000 $mg\ l^{-1}$ induces only a modest loss (0 to 6 %) of intensity for ion lines, in contrast to the much more severe matrix effects seen in ICP mass spectrometry.

Keywords: *inductively coupled plasma; ICP; secondary discharge; Mach disk; supersonic jet; echelle spectrometer; charge-coupled detectors; CCD; atomic emission spectrometry; ICP-MS.*

---

[1] *J. Anal. Atomic Spectrom.*, 1998, **13**, 223.

[2] Corresponding author.

Introduction

Supersonic jet expansions into evacuated chambers have been investigated in many different laboratories (1-4). Optical emission measurements from a reduced pressure plasma extracted from an analytical ICP were first reported by Lim et al .(5),who showed that ion lines from the supersonic jet were much more prominent than neutral atom lines. The intensities were about 1000 times lower than those observed from the normal analytical zone (NAZ) of an ICP. Ratios of ion to atom line intensity (M (II)/M (I)) from the afterglow region were similar to those observed from the NAZ of an ICP (5).The background emitted by the afterglow was much weaker than that emitted by an ICP. In a second study, the gas kinetic temperature in the Mach disk region was measured to be ~2200 K (6).

Previous basic studies of the extraction process for ICP-MS include optical measurements of the extracted gas (7), photographic studies (8), gas dynamics (9), electron density measurements (10), and use of an extraction chamber with an echelle spectrometer and two CCDs (11). In addition, Borer and Hieftje evaluated the performance of a microwave-boosted reduced-pressure plasma extracted from an atmospheric pressure ICP (12-14).

In the present paper, the primary objective is to intensify emission from the extracted plasma without increasing the background noise substantially. These measures should improve detection limits compared to those seen previously (11). The eventual objective of this research is to devise a multielement emission source that produces spectra like those from the ICP itself without the intense continuum background, so that the low dark current of the CCD can be exploited. The present work describes the effect of a mild secondary discharge between the

plasma and the sampling orifice (15) on optical emission from the extracted plasma. This discharge is strongest at low power, high aerosol gas flow rate, and high water load (15-19). The discharge also becomes more intense as the sampler is retracted further downstream in the plasma. A mild discharge is expected to accelerate electrons during the extraction process, increase electron temperature (10), and enhance excitation by electron-neutral or electron-ion collisions in the Mach disk. Such collisions should thus enhance the intensities of various emission lines.

Experimental Section

A schematic diagram of the extraction chamber used in this work is shown in Figure 1. Table 1 summarizes the instrumentation and operating conditions.

ICP Instrumentation The plasma was generated using an external RF generator and matching network, rather than the one supplied with the instrument, for reasons described below. The matching network was mounted on an xyz translation assembly. The torch was turned to the horizontal orientation. The load coil was grounded at the downstream turn to the shielding box, while the other end was connected to the RF output of the matching network (15). Analyte was introduced into the ICP by a concentric nebulizer (Model TR 30C3, Meinhard Associates, Santa Ana, CA) with a Scott type spray chamber (20) followed by a desolvation system (21).

Extraction Chamber The extraction system (Figure1) is described in detail in previous publications (5,6,11), and consists of a horizontal ICP that is sampled through a 1.06 mm

diameter circular orifice drilled in a water-cooled copper disk. On the outside of the plate is a quartz cylinder used as the wall of the extraction chamber. The quartz chamber is sealed to the sampling plate with a Viton gasket. The other end of the quartz chamber is sealed to a pumping flange, which is connected to a rotary pump. The copper flange with the orifice was grounded with copper tubing, which also provided cooling water. An inline valve was used to control the pressure in the extraction chamber. The extraction chamber was centered on the ICP. It should be noted that copper emission lines from the sampler were not observed, and the diameter of the sampling orifice did not expand noticeably over a one month period, which indicates the secondary discharge is not strong enough to sputter copper from the sampling orifice.

Optics and Detection A Perkin Elmer Optima 3000 echelle spectrometer (Norwalk, CT, USA) with a segmented array charge-coupled device detector (22,23) was used for this experiment. This device provides high quantum efficiency in the UV, low dark current, low read out noise, and simultaneous multielement capability.

The generator and coupling box were the same ones used in our initial experiments concerning emission from the Mach disk (5,6). An external RF generator was necessary because the one supplied with the Optima did not produce a noticeable secondary discharge, as noted previously (11). The plasma supplied with the Optima was intended for use with a "free" ICP, i.e., one without a sampling orifice present and was not designed to either produce or suppress a secondary discharge.

As can be seen in Figure 1, the extracted plasma is well outside the shielding box of the Optima. To transmit light into the Optima, a quartz lens (f/7) produced a focused image (magnification 1) of the extracted plasma onto the usual position of the torch inside the shielding box of the Optima. This image was then transferred by the entrance optics provided with the Optima. The plasma was blocked by a black metal shield, and the experiments were performed in a dark room to minimize stray light. The section of the extracted plasma viewed is shown in Figure 2b. The vacuum chamber was grounded carefully to alleviate RF interference.

Reagents Analyte solutions were prepared by serial dilution of concentrated stock solutions. For Ca, Sr, Mn and Mg, ICP single element stock solutions (Plasma-Chem, Farmingdale, NJ, USA) with analyte concentrations of 50 mg l^{-1} in 2% (v/v) aqueous HNO_3 (J.T.Baker, Phillipsburg, NJ, USA) were used. Solid sodium chloride (analytical grade, Aldrich, Milwaukee WI) was dissolved into the HNO_3 solutions for the matrix effect studies.

Results and Discussion

Structure of the Extracted Jet The extracted plasma and shock waves behind the sampling orifice are shown schematically in Figure 2. With the inline valve open, the pressure is 133 Pa (1 torr, Figure 2a). The jet consists of the zone of silence surrounded by a faint, diffuse barrel shock and Mach disk. There is no visible emission from inside the zone of silence. The barrel shock and Mack disk are caused by collisions between fast atoms from the supersonic jet and the background gas. The collisions reheat and scatter the atoms and induce emission.

At a pressure of 1000 Pa (7.5 torr, Figure 2b), the visible structure of the expansion becomes more compact and intense, as described previously by Gray (8). A second barrel shock and Mach disk form; each is only about 3 mm diameter. Outside the orifice, a dark space about 6 mm in diameter surrounded by a pale blue ring is observed (7). This ring is probably generated by an RF potential from the ICP induced between the two metal plates of the extraction chamber.

Effect of Sampling Position on Emission from Mach Disk In this study the Mach disk was first located by spatially profiling emission from the extracted plasma. At 7 mm from the sampling orifice, maximum emission was observed from the Mach disk region for various emission lines. Theoretically, the location of the onset of the Mach disk is given by the following equation (24):

$$X_m/D = 0.67\,[P_0/P_1]^{1/2} \quad \text{..... (1)}$$

where X_m is the distance of the Mach disk from the sampling orifice, D is the diameter of the sampling orifice (1.06 mm), P_0 is the ICP pressure (10^5 Pa, 760 torr) and P_1 is the background pressure in the extraction chamber. The orifice used here was 1.06 mm in diameter and the pressure in the extraction chamber was 1000 Pa (7.5 torr), which should produce the first Mach disk at $X_m = 7.05$ mm, in good agreement with the observed maximum in emission intensity at 7 mm.

The variation of net intensity of various atom (I) and ion (II) lines with sampler-load coil separation (i.e., sampling position) at constant chamber pressure (1000 Pa, 7.5 torr), aerosol gas flow rate (1.1 l min^{-1}) and power (1.1 kW) is shown in Figure 3. This experiment is performed by moving the plasma relative to the sampler and observation region, which are fixed relative to

the spectrometer. Moving the plasma changes both the plasma region sampled by the vacuum chamber and the severity of the secondary discharge.

As shown in Figure 3, the line intensities maximize when the sampler is 15 to 17 mm from the load coil. The spatial emission profile for Ca (I) 422.673 is double humped, with the main peak at 16-17 mm and a weak one at 25 mm. The profiles of the other lines studied (Ca (II), Mg (I), Mg (II), Sr(I), Sr (II), Mn (I), Mn (II)) have a single hump shape with maximum intensity at 15-17 mm. A mild secondary discharge can be seen between the plasma and the sampling cone at a sampling position of 15 mm or further from the load coil. The discharge in the present work is visually much weaker than that described previously for enhancing emission intensity outside the sampler in the ICP (15-19).

Effect of Power The variation of line intensity with power at constant sampling position (15 mm), aerosol gas flow rate (1.0 l/min) and pressure (7.5 torr) is shown in Figure 4. The Ca (I) line (422.676 nm) maximizes at low power (0.9 kW). Strontium atom (I) and ion (II) lines reach maxima at 1.2 kW. The Mg (I) line intensity maximizes at 1.2 kW and then plateaus off as power increases further. This plateau might be due to the fact that as power increases the strength of the discharge decreases (15). Meanwhile, the intensities of the Mn atom and ion lines increase similarly as forward power increases. A power of 1.2 kW is suitable for multielement work with only a minimal compromise in signal, especially for ion lines, as is the case when emission is observed from the ICP itself.

Effect of Aerosol Gas Flow Rate The effect of aerosol gas flow rate on analyte net intensity from the Mach disk at constant sampler load coil separation (15 mm), forward power (1.2 kW) and pressure (7.5 torr) is shown in Figure 5. The profile of analyte ion line intensity as a function of aerosol gas flow rate is a single hump with a maximum located between 1.0-1.1 l min^{-1}. The profiles for analyte atom lines are different from those for ion lines. The plots for Ca (I) and Sr (I) lines have two humps at 1.0-1.2 l min^{-1} and 1.6 l min^{-1}. The second hump appears at 1.4 l min^{-1} for the Mg (I) line. Surprisingly, the profiles for both Mn (I) and Mn (II) lines are single sharp peaks with maxima at 1.2 l min^{-1}.

Presumably, the number density of metal ions (M^+) and excitation temperature (T_{exc}) are related to the corresponding quantities outside the sampler in the ICP (11). Thus, the intensity of metal ion lines from the Mach disk can be generalized by the following proportionality (11):

$$(I_{M+})_{MD} \propto (n_{M+})_{MD} \exp(-E^*/kT_{exc}) \quad \text{..... (2)}$$

where MD refers to the Mach disk, E^* is the excitation energy (measured relative to the lowest level of the ion), and k is the Boltzmann constant.

The data presented in Figure 5 can be rationalized from combining this proportionality with the concept that the section of the axial channel that passes through the orifice and the severity of the secondary discharge both change with aerosol gas flow rate. When the aerosol gas flow rate is 1.1 l min^{-1} and sampling position is 15 mm, the discharge is visible outside the sampler. The potentials that accompany this mild discharge accelerate electrons during the extraction process, which increases electron temperature, T_{exc}, and the fraction of excited M^+ ions in the Mach disk. Furthermore, at this sampling position the tip of the initial radiation zone (IRZ) (25) is about 1 - 2 mm upstream from the sampling orifice. This is roughly the same sampling

position that maximizes ion signal in ICP-MS (26-27). Thus, ion lines in particular are enhanced at 1.1 l min^{-1}.

At low aerosol gas flow rate (~ 0.5 l min^{-1}), less total analyte reaches the plasma, the sampler is too far downstream from the IRZ, and the sampler is at a position where the analyte stream has spread out considerably. The secondary discharge is still present but too weak to be visible, as is the case with most ICP-MS devices that do not employ a balanced or shielded load coil. Thus, both the density factor n_{M+} and the Boltzmann factor in eqn. 2 are reduced, and emission intensity is low. At extremely high aerosol gas flow rate (1.6 -1.7 l min^{-1}), the discharge is strong but the sampling orifice is well inside the IRZ, where there are few M^+ ions. These conditions produce highest emission from neutral atoms at the expense of ion emission.

Ion to Atom Line Intensity Ratios The figures discussed to this point are intended primarily for optimization purposes and therefore show only normalized intensities. The effect of the secondary discharge on ion/atom intensity ratios is presented in Table 2. In general, the ion/atom intensity ratios from the Mach disk generated in the present work were higher than those seen with the Mach disk produced using the plasma supplied with the Optima, except for the intensity ratio Ca(II) 396.847 / Ca (I) 422.673, which is perhaps a bit lower in the present work. This enhancement in ion line intensity is attributed to the fact that a mild discharge accelerates electrons during the extraction process, which increases electron temperature (T_e) and T_{exc} in the observed region of the extracted plasma, as described above.

Mermet (28) suggests the use of the intensity ratio Mg (II) 280.270 nm/Mg (I) 285.213 nm as a simple test of the "robustness" of atomization and excitation conditions in an ICP. This

ratio should be ~10 if the plasma is operated under "robust" conditions. In our experiment, this intensity ratio is 4.5 (Table 2). It should be noted that intensity ratios measured in this study can not be directly compared to those values observed from the NAZ of an ICP (29) due to the variable sensitivity of different subarrays in the CCD. These two Mg lines are detected on different subarrays. Different lines are also measured in different orders in the echelle configuration, which also complicates comparison with ion/atom intensity ratios determined using other instruments. Thus, the Mg (II)/Mg(I) intensity ratio observed with our particular Optima from the normal analytical zone of an ICP is approximately 3.7. The value of 4.5 shown in Table 2 from the Mach disk is actually higher than that seen from the ICP itself with our particular spectrometer, in agreement with our earlier observations(5,9). We therefore conclude that the Mach disk is at least as "robust" as the ICP in the Optima, according to Mermet's criterion.

Detection Limits The limit of detection (LOD) is defined as the concentration necessary to produce a net signal equivalent to three times the standard deviation of the background. The LODs obtained in this study are shown in Table 3. Standard deviation (σ) was calculated for 11 consecutive measurements with an integration time of 200 seconds for each line. The values are measured for the most intense line for each element under the multielement operating conditions listed in Table 1. Detection limits in the range 0.1-2 $\mu g\ l^{-1}$ were obtained.

The LODs obtained in the present work are better than the range of 2-6 $\mu g\ l^{-1}$ previously obtained by Shen et al. (11). The reasons are illustrated by the data in Table 4, which shows the

effect of the secondary discharge on sensitivity, background, noise and detection limits. In general, the mild discharge enhanced analyte line intensity by factors of 20 to 40, even though use of the external RF generator forced us to put the Mach disk a substantial distance from the entrance slit (see Figure 1). Thus, the light throughput is probably poorer in the present work than in that reported previously (11), when the vacuum chamber was inside the usual shielding box of the Optima.

Meanwhile, the secondary discharge increased the background by factors of 10 to 20. The increase in background is presumably due to the stronger white continuum emission from the Mach disks and also to the blue ring around the plate containing the sampling orifice (see Figure 2). The blue ring is prominent only when there is a substantial secondary discharge.

Although the background emitted by the Mach disk is elevated twenty fold by the secondary discharge, the noise on the background is not changed appreciably. Thus, detection limits for the elements studied are better than those obtained by Shen et al (11). while viewing the Mach disk without the secondary discharge. Our new detection limits are also about the same as those obtained by the Optima 3000 during lateral viewing of the ICP alone (30).

Effect of Sodium Matrix on Analyte Line Intensity The effect of sodium concomitant on analyte signals is shown in Figure 6. The optimized operating conditions described above were used for these experiments and are identified in the figure caption. Blanks of the most concentrated matrix solutions were analyzed and did not have significant amounts of the analytes.

The two plots at the top of Figure 6 show that the intensity of the Ca (II) line at 393.366 nm is not affected substantially by the Na matrix at concentrations up to at least 10,000 mg Na l^{-1}, i.e., a 1% Na solution. The intensity of the Ca (I) line at 422.673 nm is suppressed by about 15% at 10,000 mg Na l^{-1}. For both Mg (II) and Mg (I) lines, an odd enhancement is seen at 1000 mg Na l^{-1}, followed by a modest suppression of signal. The behavior of strontium signal with sodium concentration is erratic. For Sr (II) 407.771 nm, the various points average to a modest suppression of about 10%, whereas the Sr (I) line is enhanced in the presence of the Na matrix. It is odd that the sodium matrix should enhance the intensity of the Sr (I) line and suppress that of the Ca (I) line.

For the ion lines and the relatively high energy neutral atom line Mg (I) 285.213, the matrix effects shown in Figure 6 are similar in magnitude to those that would be expected if emission were observed from the ICP alone under multielement operating conditions (15). These are the most sensitive lines for these elements and would be the preferred ones for analytical use.

The matrix effects shown in Figure 6 are comparable to those seen in the early work of Lim and Houk (5) and are much less severe than those that would be seen by ICP-MS (31). We suggest that the moderate severity of the matrix effect in the present work is the result of juxtaposition of two competing phenomena. Sodium at these concentrations would be expected to cause a substantial loss of analyte ions in the plasma itself, according to the measurements of Hobbs and Olesik (31). It is difficult to estimate the extent of loss of analyte ions directly from their data, since a) they report results for Li and Ba but not for a Na matrix itself, and b) the plasma they used did not have a sampling orifice present.

Nevertheless, sodium at 10,000 mg Na l^{-1} should suppress the analyte ion density in the ICP by at least a factor of two. Taken alone, this effect should then suppress the signal for analyte ions from the Mach disk.

Some opposing phenomenon must then excite the ions more efficiently to offset this expected loss of analyte ions. Hieftje and co-workers report Thomson scattering measurements that show that T_e along the central axis of the ICP actually increases when an alkali metal matrix is added (33). Previous Langmuir probe measurements show that changing plasma conditions that increase the plasma potential and intensity of the secondary discharge cause a corresponding increase in T_e in the supersonic jet (10,34). Thus, addition of sodium could increase electron temperature in both the plasma and in the Mach disk. The presence of more energetic electrons in the Mach disk should boost the populations of excited levels of analyte ions and thus compensate for the expected suppression in analyte ion density. Since this second process primarily produces a higher fraction of ions in excited states, rather than more total ions, it does not influence matrix effects in ICP-MS, which are substantially more severe than those seen in the present work.

Conclusion

The present work shows that inducing a mild secondary discharge improves detection limits by increasing line intensities without also increasing the noise on the background. Additional improvements in detection limits could therefore be possible if the intensities could be boosted further. The Mach disk source also benefits from similar tolerance to matrix effects induced by sodium as the ICP itself. However, the detection limits in the

present work are improved only to the point where they are comparable to those obtained from conventional lateral viewing of the ICP, i.e., they are not yet competitive with the performance of axially-viewed ICP emission spectrometry or ICP-MS. It must also be admitted that the lines measured are relatively easily excited. Thus, although the Mach disk emission source shows some promise, further development is necessary before it represents any improvement over the existing ICP.

Acknowledgment

Ames Laboratory is operated by Iowa State University for the U. S. Department of Energy under Contract No.W-7405-ENG-82. This work was supported by the Office of Basic Energy Sciences, Division of Chemical Sciences. The authors thank Perkin-Elmer for the loan of the Optima.

References

1. Anderson, J.B., Molecular Beams and Low Density Gas Dynamics, Wegener, P. P., Ed., Marcel Dekker, New York, 1974, p. 1.

2. Kantrowitz, A., and Grey, J., *Rev. Sci. Instr*, 1951, **22**, 328.

3. Knuth, E. L., *Appl. Mech. Rev.*, 1964, **17**, 751.

4. Houk, R. S., Fassel, V. A., Flesch, G. D., Svec, H. J., Gray, A. L., and Taylor, C. E., *Anal. Chem.*, 1980, **52**, 2283.

5. Houk, R. S., and Lim, H. B., *Anal . Chem.*, 1986, **58**, 3244.

6. Lim, H. B., Houk, R. S., Edelson, M. C., and Carney, K. P., *J. Anal . Atomic Spectrom.*, 1989, **4**, 365.

7. Kawaguchi, H., Asada, K., and Mizuike, A., *Mikrochim. Acta*, 1988, **III**, 143.

8. Gray, A. L., *J . Anal . Atomic Spectrom.*, 1989, **4**, 365.

9. Douglas, D. J., and French, J. B., *J. Anal . Atomic Spectrom.*, 1989, **4**, 371.

10. Lim, H. B., and Houk, R. S., *Spectrochim. Act, Part B*, 1990, **45B**, 453.

11. Luan, S., Pang, H. M., and Houk, R. S., *J . Anal . Atomic Spectrom.*, 1996, **11**, 247.

12. Borer, M. W., and Hieftje, G. M., *Spectrochim. Acta, Part B*, 1991, **14**, 463.

13. Borer, M. W., and Hieftje, G. M., *J. Anal . Atomic Spectrom.*, 1993, **8**, 333.

14. Borer, M. W., and Hieftje, G. M., *J. Anal . Atomic Spectrom*, 1993, **8**, 339.

15. Gray, A. L., Houk, R. S., and Williams, J. G., *J. Anal . Atomic Spectrom.*, 1987, **2**, 13.

16. Olivares, J. A., and Houk, R. S., *Appl . Spectrosc.*, 1985, **39**, 1070.

17. Lim, H. B., Carney, K. P., Edelson, M. C., Houk, R. S., and Brenner, I. B., *Spectrochim. Acta, Part B*, 1993, **48**, 1617.

18. Houk, R. S., LaFreniere, B. R., Lim, H. B., and Fassel, V. A., *Appl . Spectrosc.*, 1987, **41**, 391.

19. Tan, H., Ishii, I., and Montaser, A., *J . Anal . Atomic Spectrom.*, 1991, **6**, 317.

20. Scott, R. H., Fassel, V. A., Kniseley, R. N., and Nixon, D. E., *Anal . Chem.*, 1974, **46**, 75.

21. Fassel, V. A., and Bear, B. R., *Spectrochim . Acta Part B*, 1986, **41**, 1089.

22. Barnard, T. W., Crockett, M. I, Ivaldi, J. C., and Lundberg, P. L., *Anal. Chem.*, 1993, **65**, 1225.

23. Barnard, T. W., Crockett, M. I, Ivaldi, J. C., Lundberg, P. L., Yates, D. A., Levine, P. A., and Dauer, D. J., *Anal. Chem.*, 1993, **65**, 1231.

24. Ashkenas, H., and Sherman, F. S., In Rarefied Gas Dynamics Proc. 4th Int . Symp . Rarefied Gas Dynamics, Ed .De Leeuw, J. H., Academic Press, New York, 1966, Vol. II, pp. 84-105.

25. Koirtyohann, S. R., Jones, J. S., and Yates, D. A., *Anal . Chem.*, 1980, **52**, 1966.

26. Vaughan, M. A., Horlick, G., and Tan, S. H., *J. Anal . Atomic Spectrom.*, 1987, **2**, 765.

27. Horlick, G., Tan, S. H., Vaughan, M. A., and Rose, C. A., *Spectrochim . Acta, Part B*, 1985, **40**, 1555.

28. Mermet, J. M. Anal. Chim. Acta 1991, **250**, 85.

29. Winge, R. K., Fassel, V. A, Peterson, V. J., and Floyd, M. A. Inductively Coupled Plasma- Atomic Emission Spectroscopy. An Atlas of Spectral Information; Elsevier: Amsterdam, The Netherlands, 1985; Appendix A.

30. Optima 3000 Wavelength Tables, Perkin-Elmer Corporation, 1993.

31. Olivares, J. A., and Houk, R. S., *Anal . Chem.*, 1986, **58**, 20.

32. Hobbs, S. E., and Olesik, J. W., *Spectrochimica Acta, Part B*, 1993, **48**, 817.

33. Hanselman, D. S., Sesi, N. N., Huang, M., and Hieftje, G. M., *Spectrochim. Acta Part B*, 1994, **49**, 495.

34. Lim, H. B., Houk, R. S., and Crain, J. S., *Spectrochim. Acta, Part B*, 1989, **44**, 989.

Table 1. Experimental components

Component	Manufacturer/ Description	Optimum operating Conditions
ICP generator	Type HFP3000D with Impedance-matching network Plasma Therm, Inc. Frequency 27.12 MHz	RF power 1.2 KW
ICP torch	Ames Laboratory construction	Aerosol gas flow rate 1.1 l min^{-1} Outer gas 15 l min^{-1} Sample uptake rate 1.0 l min^{-1}
Nebulizer assembly, Spray chamber, Desolvation apparatus (21)	Meinhard nebulizer Scot-type, uncooled spray chamber	Heating temperature 100 ^0C Condenser temperature 0 ^0C
Sampler	1.06 mm diameter circular orifice in copper disk centered on ICP	Sampling position: 16 mm from load coil on center
Pressure measurement	Convectron vacuumgauge Granville-Phillips 275	Extraction chamber pressure 1000 Pa (7.5 torr)
Vacuum pump	Edwards E2M18 Pumping speed 1.2 l s^{-1}	

Table 2. Ion/atom line intensity ratios from the Mach disk compared to those obtained without a secondary discharge[11]

Line pair, nm	**Intensity Ratio**	
	Present Work	**Previous work (11)**
Ca (II) 393.366/Ca (I) 422.673	28	22
Ca (II) 396.847/Ca (I) 422.673	3.5	4.5
Sr (II) 407.771/Sr (I) 460.733	33	22
Sr (II) 421.552/Sr (I) 460.733	10	7
Mn (II) 257.610/Mn (I) 279.482	6	*
Mn (II) 260.569/Mn (I) 279.482	3	*
Mg (II) 279.533/Mg (I) 285.213	11	4.5
Mg (II) 280.270/Mg (I) 285.213	4.5	1.5

* not measured in ref .11.

Table 3. Sensitivities (Z_a) and Detection Limits

Element and Line	Z_a counts s^{-1}	Z_b counts s^{-1}	σ counts s	Detection Limits, $\mu g\ l^{-1}$ Present work	Previous work(11)	ICP+ Optima†
Ca (II) 393.366	$1.1x10^5$	4.12	0.0694	0.10	2	0.4
Mg (II) 279.553	$2.3x10^4$	4.01	0.0705	0.4	6	0.4
Sr (II) 407.771	$6.3x10^4$	4.87	0.0425	0.1	4	0.1
Mn (II) 257.610	3250	5.11	0.0523	2	*	2

Z_a is the peak intensity of the analyte line after background correction. The analyte concentration is 50 ppm.
Z_b is the spectral background at the peak maximum
σ is the standard deviation of the blank for 11 replicates.
The detection limit is the solution concentration necessary to produce a net signal equal to three times the standard deviation of the blank.
†These values are detection limits (LOD) listed for the Optima during lateral viewing of emission from the conventional ICP.[30]
*Not measured in ref. 11.

Table 4. Effect of secondary discharge on sensitivity, background, noise and detection limits.

Element And Line	Z_a ratio	Z_b ratio	σ ratio	LOD ratio
Ca (II) 393.366	23	25	0.96	0.05
Mg (II) 279.553	11	20	0.87	0.016
Sr (II) 407.771	24	26	0.67	0.06

Z_a ratio is (net intensity with sec. discharge)/(net intensity from ref. 11, no sec. discharge). The other ratios are defined similarly.
Z_b is the net peak intensity of the spectral background at the peak maximum.
σ is the standard deviation of the blank for 11 replicates.
LOD is the solution concentration necessary to produce a net signal equal to three times the standard deviation of the blank.

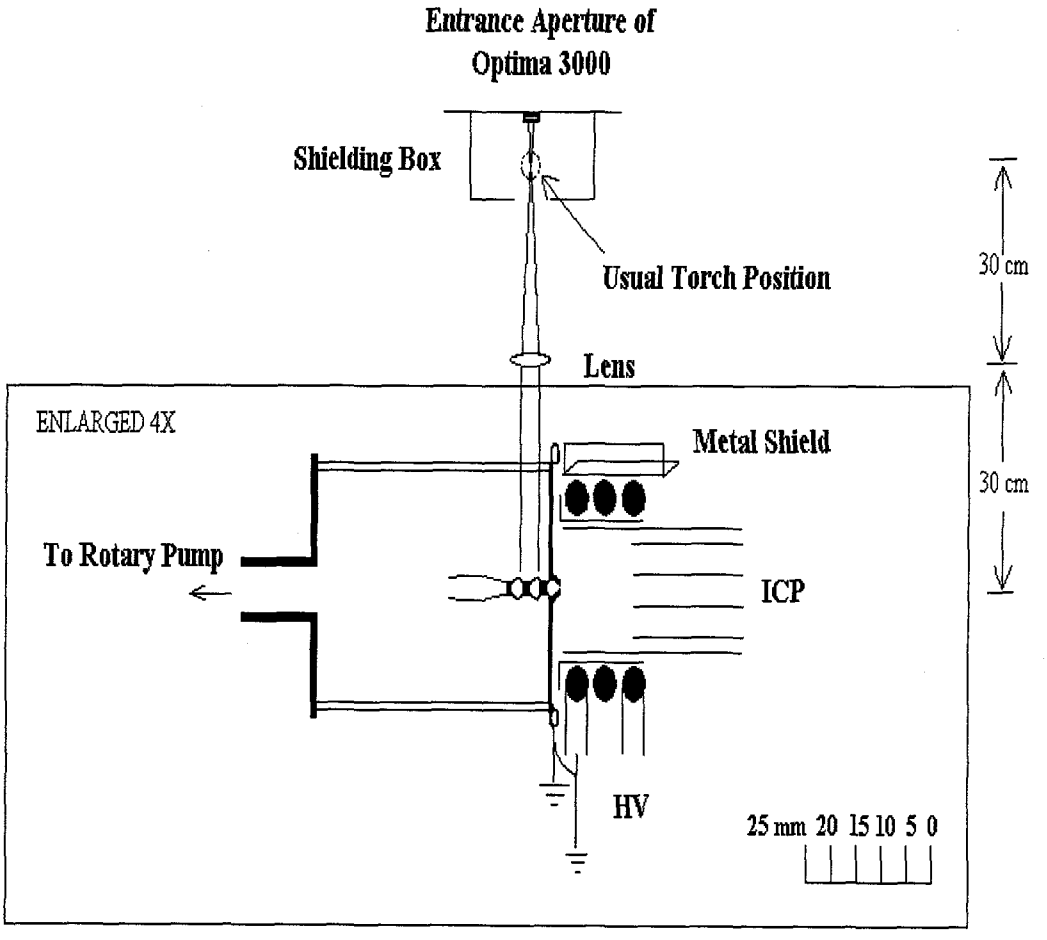

Figure 1. Schematic diagram of experimental setup. Note that the extraction chamber is to larger scale than the lens and the optical path.

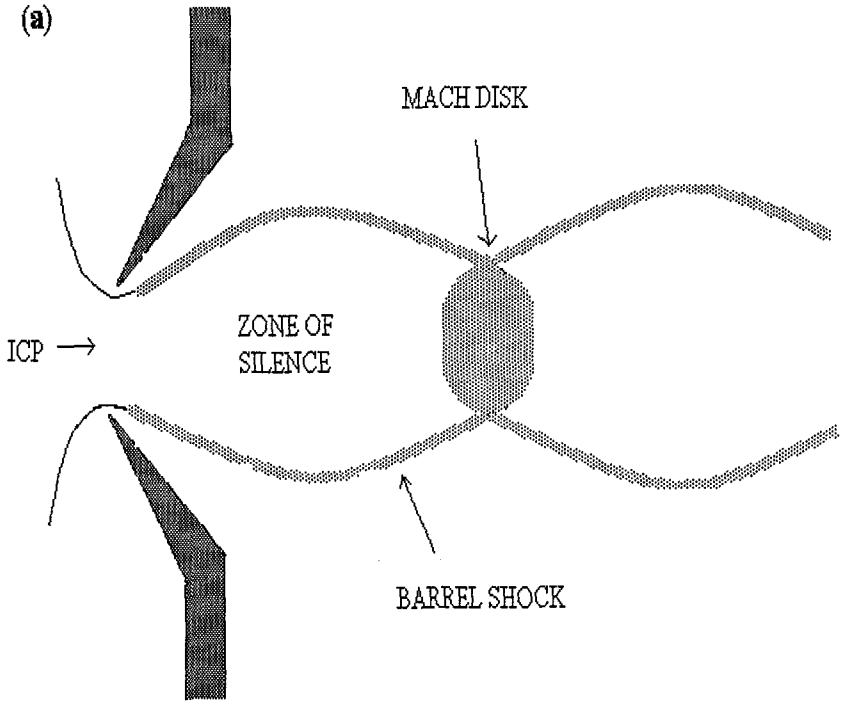

Figure 2. Close up diagram of supersonic jet and Mach disk: a) pressure = 133 Pa (1 torr), b) pressure = 1000 Pa (7.5 torr). The latter operating pressure was used in the present work.

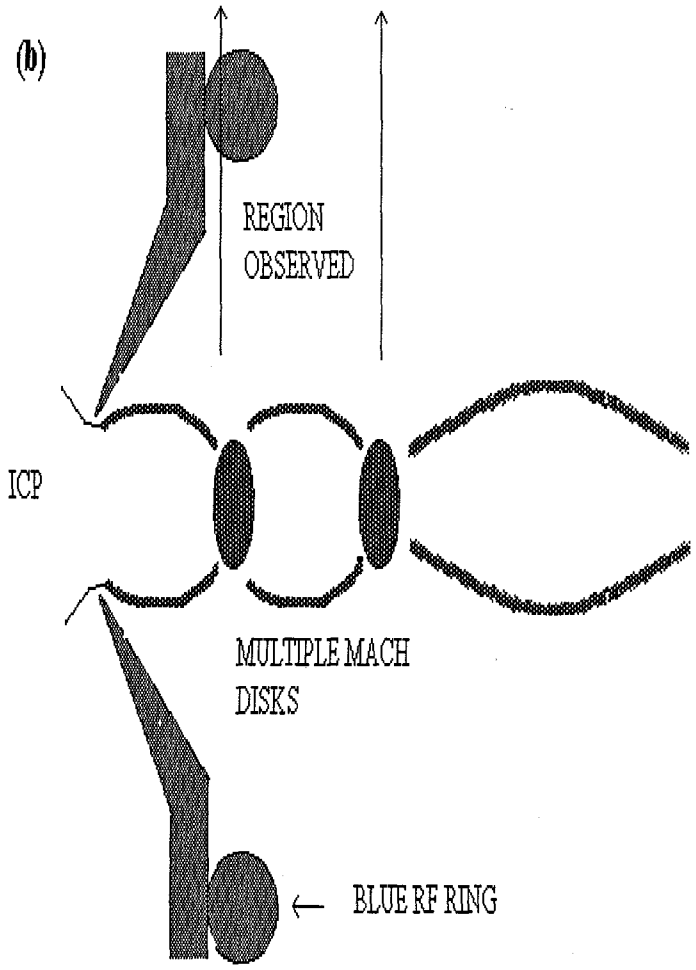

Figure 2. Cont.

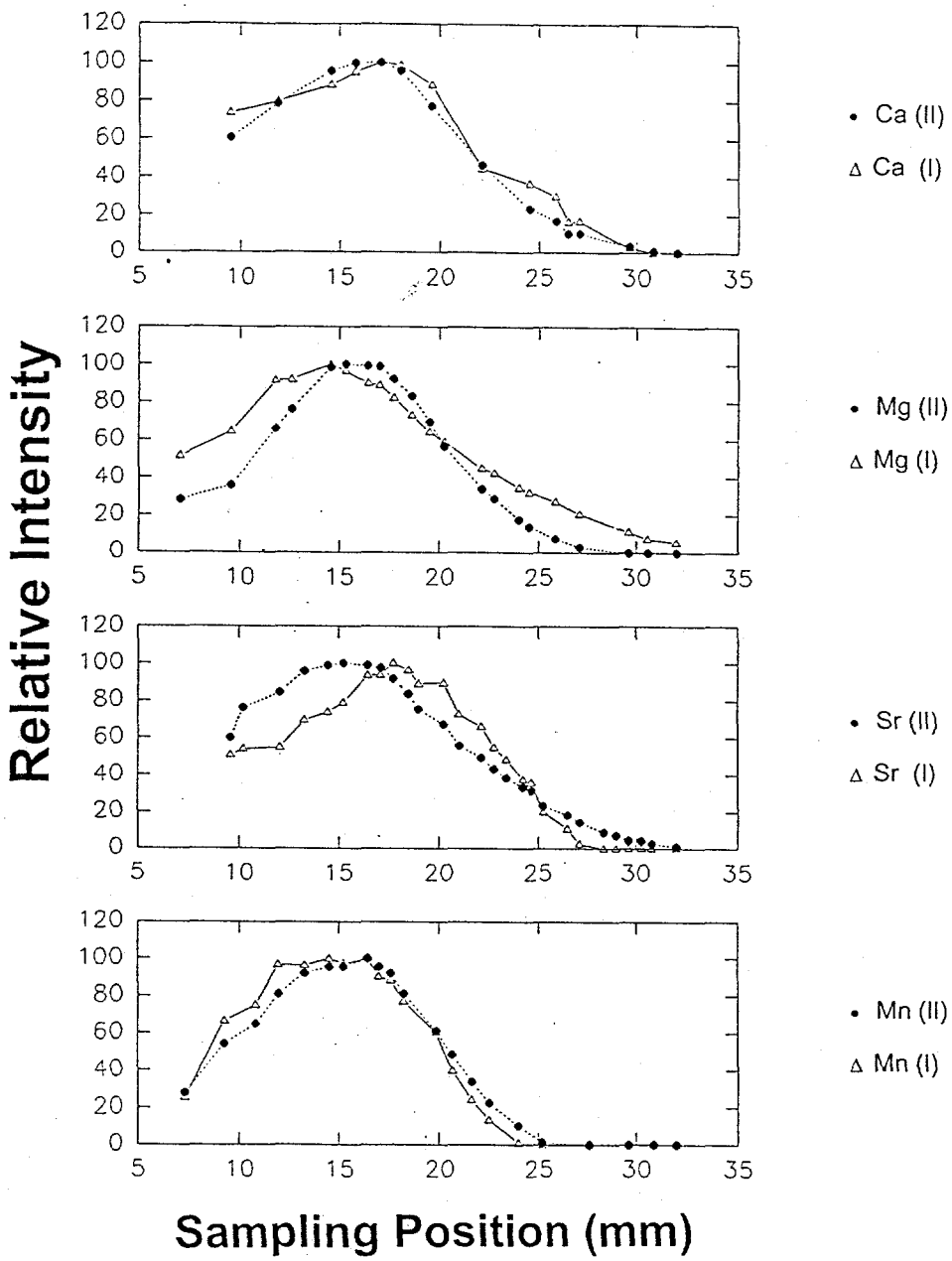

Figure 3. Effect of sampling position on emission intensity from Mach disk. Specific wavelengths are given in Table 2. The analyte concentrations were 50 mg l^{-1}, and the intensities are normalized in these and subsequent figures.

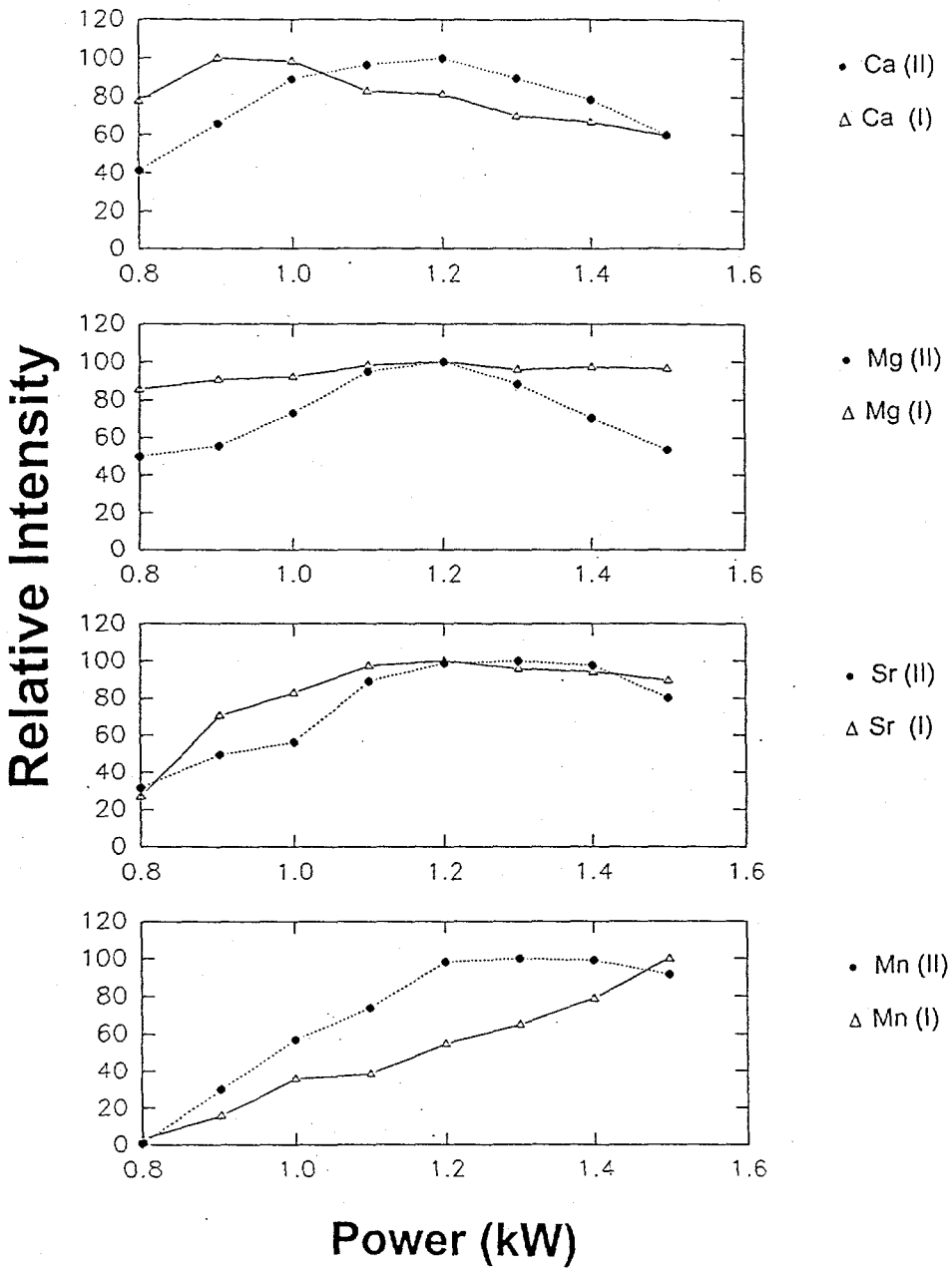

Figure 4. Dependence of analyte line intensity on power.

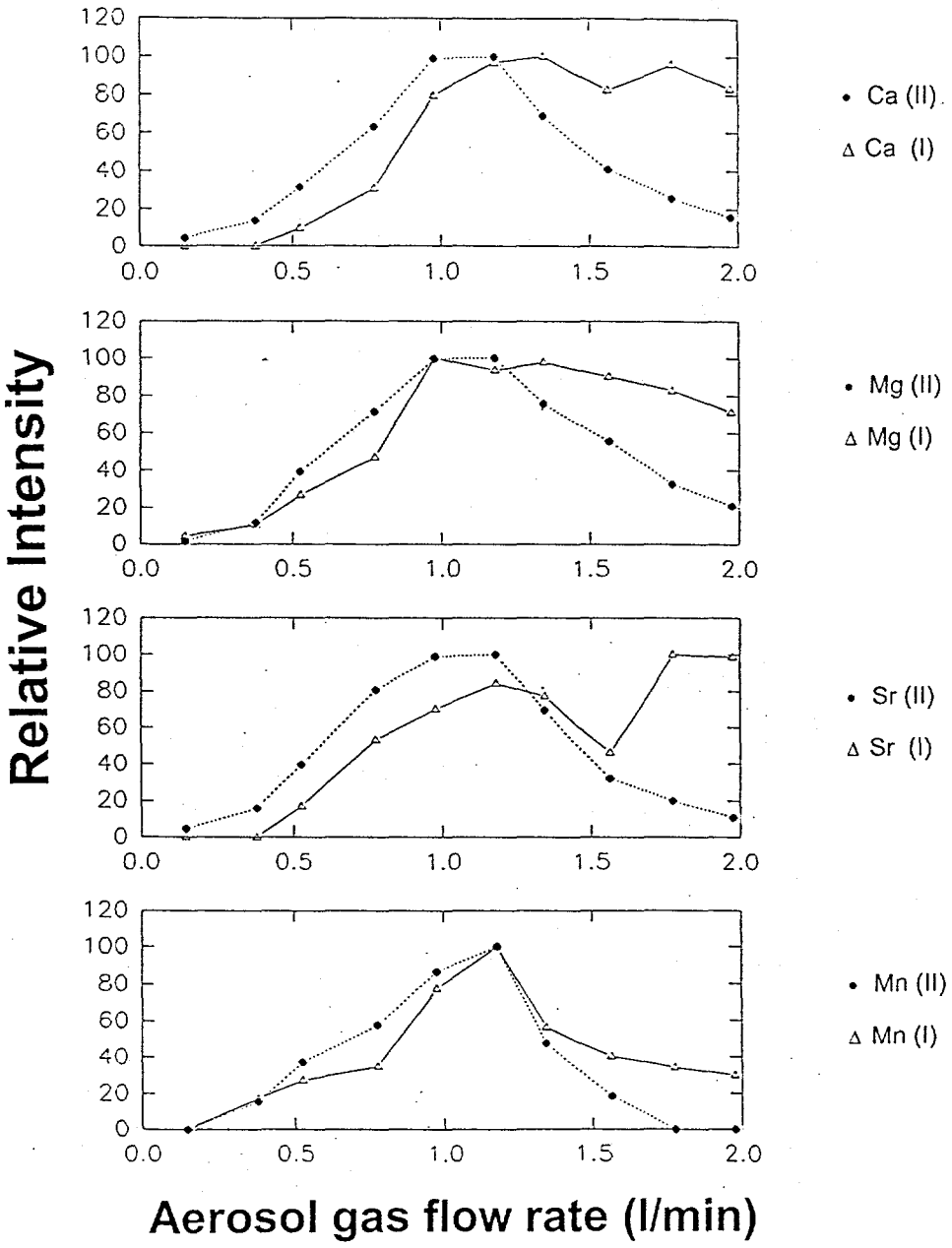

Figure 5. Dependence of analyte line intensity on aerosol gas flow rate.

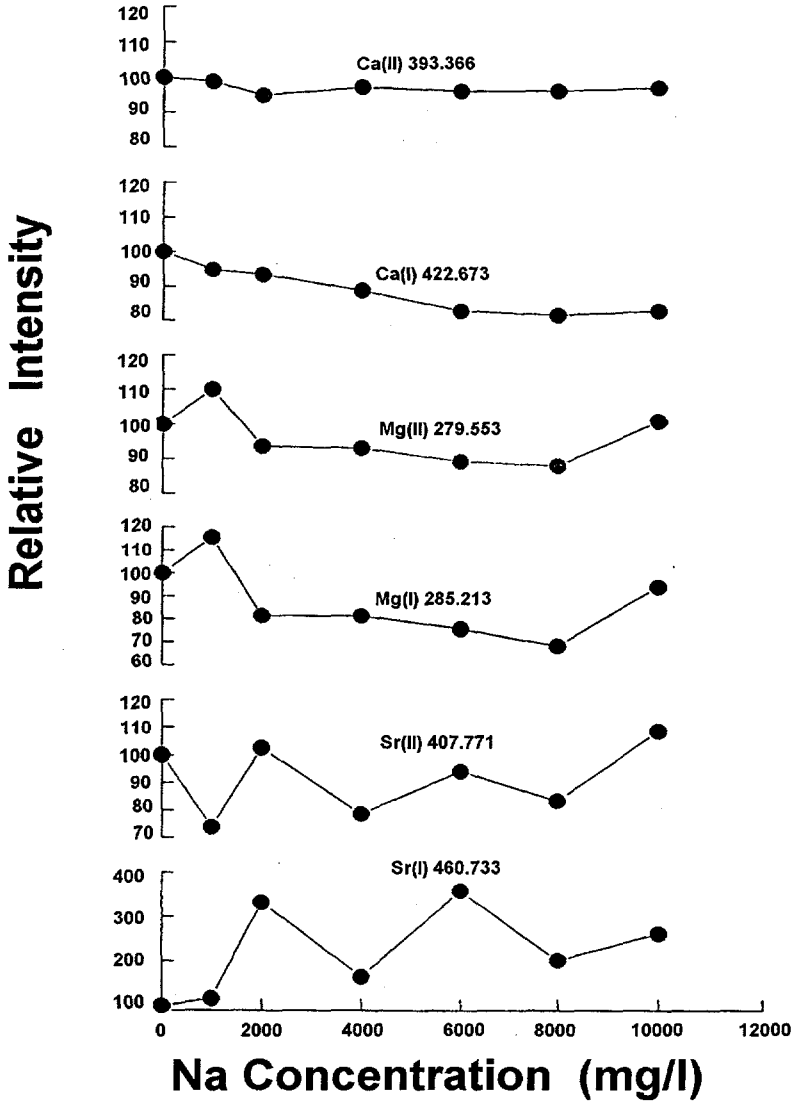

Figure 6. Effect of sodium concomitant on analyte line intensity under multielement operating conditions. The analyte concentrations were 50 mg l^{-1}

CHAPTER 3. HIGH RESOLUTION MASS SPECTROMETER WITH A MULTIPLE PASS QUADRUPOLE MASS ANALYZER

A paper published in Analytical Chemistry[1]

Ma'an H. Amad and R. S. Houk[2]

Abstract

The peak shape narrows and the resolution improves if the ions are simply reflected back and forth through a conventional quadrupole mass analyzer. CO^+ and N_2^+ at m/z = 28 are separated to 50% valley with half of the original signal remaining. These two ions can be resolved to baseline (m/Δm) = 5000 with 1% of the original signal remaining.

Introduction

Quadrupole mass analyzers are widely used for many applications such as GC-MS, LC-MS, tandem MS with a triple quadrupole, ICP-MS and residual gas analysis. These devices are generally limited to unit mass resolution; they usually cannot separate chemically different ions at the same nominal m/z value. A high resolution device such as a magnetic sector or Fourier transform – ion cyclotron resonance instrument can resolve such pairs of interfering ions and can determine the elemental formula of an organic compound from accurate measurements of the m/z value of the parent ion. High-resolution selection of the

---

[1] *J. Anal. Chem.*, 1998, **70**, 4885.

[2] Coresponding author.

parent ion in the first stage of a tandem MS also greatly improves the selectivity of a particular parent ion – daughter ion channel in collision induced dissociation for analysis of complex mixtures. If the resolution of a quadrupole could be improved, then such measurements would be possible without the additional size, complexity and expense associated with the usual type of high-resolution mass analyzer.

The resolution R achievable with a particular quadrupole is typically adjusted via the DC/RF voltage ratio and is ultimately limited by the mechanical accuracy with which the rods are constructed and supported (1-3):

$$R = m/\Delta m \qquad (1)$$

where m = m/z value of the ion measured and Δm = peak width at some specified fraction of the peak height (often 50% or 10%). Abundance sensitivity is another important indication of the ability of a mass analyzer to separate different ions. This parameter is basically the ratio of [signal for a peak at m/z]/[signal at (m/z - 1) or (m/z + 1)]. To borrow terminology from chromatography, the abundance sensitivity is a measure of the fronting (i.e., at m/z – 1) or tailing (m/z + 1) of a mass spectral peak and is determined largely by the RF frequency and the mechanical quality of the rods. The following discussion concentrates mainly on resolution.

For a given quadrupole, the resolution R should be roughly proportional to the square of the number of RF cycles n the ions spend inside the rods:

$$R \propto n^2$$

$$m f^2 L^2 / z V_z \qquad (2)$$

where f = frequency of RF voltage applied to the rods, L = length of rods, z = ion charge and V_z = potential drop between source and mass analyzer, i.e., zV_z is the ion kinetic energy inside the mass analyzer (1). In practice, the resolution is also dependent on other factors such as ion injection conditions and the quality of the rods, but Eqn. 2 provides a useful basis for discussion. In particular, the resolution should increase with n^2, so there should be substantial room for improving resolution if the number of RF cycles n can be increased significantly.

The obvious ways to increase n and the associated problems are as follows:

1. Increase L – This was investigated by von Zahn (4), who constructed a rod set that was 5.8 m long and was designed to provide a resolution of 16,000. In general, however, increasing L makes the rods larger and heavier, which defeats the advantages of small size. Long rods require more electrical power; they are also much more difficult to construct and mount with the required dimensional tolerance (∓10 μm or better).
2. Increase f – For a given rod diameter, the maximum m/z value that can be transmitted decreases as f increases, so increasing frequency compromises mass range. In applications such as ICP-MS, where atomic ions are used and mass range is not much of an issue, improvements in abundance sensitivity have been reported by increasing the RF frequency (5).
3. Inject ions with low V_z – Slow ions are injected less efficiently and stay longer in the fringe fields at the entrance and exit of the mass analyzer. Even the analyte ions that are stable inside the rods are deflected by the weak DC and RF potentials in the fringe fields, which compromises transmission and causes mass discrimination (1).

The resolution achievable with a quadrupole can also be improved by operating the device in an alternate stability region, i.e., a combination of RF and DC voltages in a completely different regime than the one usually employed. These regions may be identified by the (a,q) values that provide stable ion motion (6), where a α (DC voltage)/ m/z and q $\propto$ (RF voltage) / m/z. For example, Ying and Douglas demonstrated a resolution of 9000 using Region II ($a \approx 0.03$, $q \approx 7.5$), which was sufficient to separate $^{56}Fe^{+}$ from $^{40}Ar^{16}O^{+}$ in ICP-MS experiments (2). Douglas' group also showed that operation in Region III ($a \approx q \approx 3$) provides very high abundance sensitivity (3). Other investigators have either observed or predicted similar improvements in performance (7-10). The use of alternate stability regions is accompanied by disadvantages in some cases, i.e., operation in Region II requires higher RF power and also transmits ions at high m/z that are inside Region I.

Another way to improve resolution is described by de Maack et al (11) and Beaugrand (12). These workers achieve resolution of 10,000 using "a periodically over-resolving modulation," which amounts to an additional RF potential of lower frequency and amplitude applied to the rods. This extra AC component improves resolution by creating additional subregions of the stability within the usual triangular stable region used for mass resolution, as described by Mitseski (13).

The present work presents initial results that suggest that resolution can be improved by simply reflecting ions back and forth through a quadrupole operated in the usual stability region. Even only three passes would increase L and n by a factor of three, so resolution should improve by a factor of $3^2 = 9$ (Eqn. 2). Techniques for reflecting ions are highly

developed with the reflectrons used in time-of-flight MS (14,15) and with the ion trapping detector for large biological ions described by Benner (16). Enke, Watson and co-workers (17) and Beaugrand and co-workers (18,19) reflected ions through an RF-only quadrupole collision cell to increase their opportunity for ion-molecule reaction or collision-induced dissociation. Marshall and co-workers (20) also described a linear ion trap for Fourier transform ion cyclotron resonance MS in which ions are reflected back and forth through a quadrupole structure inside an axial magnetic field.

To the best of our knowledge, the present work is the first detailed report in which ions are reflected repetitively through or trapped inside a quadrupole mass analyzer to improve mass resolution. Steiner (21) has also described experiments in which ions were trapped inside a quadrupole mass filter for this purpose. In a sense, the ion reflecting concept described in this paper is also analogous to the methods developed by Cooks and co-workers (22) to obtain high mass resolution with a quadrupole ion trap by scanning the ions out slowly so they reside in the RF fields inside the trap longer and experience as many RF cycles as possible. The main question pertains to the severity of signal loss accompanied by injecting the ions repetitively through the fringe fields, which can cause ion losses and mass discrimination for only a single pass.

Experimental Section

Instrumentation The objective of the present study is to test the feasibility of improving mass resolution by reflecting ions through a quadrupole without constructing a special device to do so. A standard triple quadrupole MS (Finnigan TSQ 4500, Figure 1) is used because it

contains a stack of convenient ion lenses at the entrance and exit of the first mass analyzer. The second and third quadrupoles are used in RF only mode. Ions are produced from gaseous samples by electron impact with an electron energy of 70 eV and a repeller voltage of +15 volts. The starting value of resolution and peak shape are adjusted and the m/z range is calibrated with the first quadrupole operated in the usual, single pass mode with DC voltages on the ion lenses.

As shown in Figure 1, square wave voltages are then applied to one lens at the entrance and one at the exit of the first quadrupole (Q1). These square waves are of equal amplitude and opposite polarity and are produced from a function generator that drives a 20X voltage amplifier with two outputs, one inverted and one non-inverted. The rise and fall times of the square waves are 86 and 56 ns, respectively.

The mass spectrum is generated by scanning the DC and RF voltages applied to the quadrupole in the usual way. This scanning process is much slower (≈ 5 s Da^{-1}) than the frequency of the reflecting wave forms. Four such scans are averaged to produce the spectra shown below. The amplitude ($\approx$360 volts p-p) and frequency (1/12 μs $\approx$ 83.3 kHz) of the square waves are adjusted until the spectrum has the desired peak shapes and resolution; Figure 1 simply cites generic values for these parameters. Spectra are acquired and processed with a commercial data system (Prolab).

The timing diagram at the bottom of Figure 1 illustrates the reflecting function of these two lenses V_1 and V_2. Ions from the source are injected while the entrance lens V_1 is negative. These ions travel to the right through Q1 until they are reflected backward by the positive voltage applied to the exit lens V_2. They then travel back toward the source.

Meanwhile, V_1 changes to +180 volts, which reflects the ions a third time. It is not known precisely how many times the ions are reflected before they escape to the detector.

Samples Cylinders containing CO or N_2 (99.995% purity) were obtained from Air Products. Perfluorotributylamine (FC-43) was obtained from Scientific Instrument Services.

Results and Discussion

Results with Open Circular Apertures In the first experiments, the reflection lenses V_1 and V_2 are the open circular apertures supplied with the device (Figure 1). The spectra are shown in Figures 2 and 3. In Figure 2, the upper panel shows the conventional spectrum obtained after only one pass. A mixture of CO^+ and N_2^+ produces only one peak. The lower panel shows the spectrum when the reflecting square waves are applied. The conventional resolution setting, i.e., the ratio of RF/DC voltages applied to the rods, is *not* changed. A valley appears between the two peaks, and the leftmost peak disappears when the CO is removed from the ion source, which shows that these peaks are from CO^+ and N_2^+ and that they have been partially separated. The two ions differ by $\Delta m = 0.01123$, and they are almost separated at half height. The numerical value of resolution in Figure 2 is $m/\Delta m \sim 2200$ (50% valley).

In Figure 2 the peak heights in the high resolution spectrum are almost half those in the low resolution spectrum. Thus, reflecting the ions has improved the resolution without causing a tremendous loss in transmission in this case.

The m/z scale is calibrated in the usual way with ions from known samples sent through the quadrupole for only one pass. When the reflecting voltages are used, the apparent m/z

values of the peaks increase by approximately 1 Da. Of course, the actual m/z value of the ions has not changed, but the DC and RF voltages that let them through the rods are slightly higher when the quadrupole is used in the reflecting mode. The high resolution spectrum in Fig. 2 shows the peaks shifted back to their correct m/z values. The reasons for the shift in m/z scale are not clear at this time. However, the m/z scale for a quadrupole mass analyzer is always established by empirical calibration anyway. Apparently, separate calibrations may prove necessary for low and high resolution. Peaks in subsequent high-resolution spectra have also been shifted back to the correct m/z value.

Similar improvements in resolution are found for other ions, like $C_3F_5^+$ (m/z = 131) and $C_4F_9^+$ (m/z = 219) from perfluorotributylamine (Fig. 3). The nominal value of resolution for the reflected ions at m/z = 219 is $m/\Delta m = 3400$ at 50% valley. The peak height is approximately 30% of that at low resolution.

Results with Grid Reflecting Optics With the open circular apertures, many of the spectra have a plateau on the low mass side of the high resolution peak. Such a plateau is evident by the elevated baseline between points a and b in Figure 2. The width of the plateau and the adjacent high-resolution peak together are about the same width as the base of the original, low resolution peak in the upper frame of Figure 2. We therefore believe the plateau is caused by ions that escape after only one pass.

To remove these "stray" ions, the open circular apertures V_1 and V_2 in Figure 1 were replaced with grids (45 mesh lines cm^{-1}, wire diam. 0.28 mm). The spectra in Figure 4 resulted. Most of the plateau is indeed removed, and CO^+ and N_2^+ are separated to baseline.

The numerical value of m/Δm improves to 5000 (50% valley), although the ion transmission is only ~ 1% of that at low resolution. Douglas and co-workers report a similar sacrifice of transmission for resolution in their experiments with alternate stability regions(2,3).

We offer the following tentative explanation for these observations. The grids remove the plateau by restricting the size, especially the length, of the reflected ion packet, so that all ions are reflected and none get out after only one pass. Unfortunately, the reflected ion packet becomes so small that only a small fraction of the ions survive. In contrast, the open lenses reflect a longer packet of ions and thus have better transmission, but they allow some ions out after only one pass.

Some satellite peaks are evident on the high mass side of N_2^+ in the high resolution spectrum in Figure 4. The reasons for these peaks are also unclear. They tend to be most noticeable when the sample is a mixture of ions close in mass, rather than a single component. It is interesting to note that overresolving modulation described by de Maack et al. (11), Beaugrand (12), and Mitseki (13) also produces satellite peaks and can shift the main peak to a higher m/z value, so the application of the reflecting AC voltage to the lenses in the present experiment may also interact with the m/z resolution function of the RF voltage applied to the quadrupole rods.

Finally, the slopes of the sides of the peaks in Figures 2-4 are about the same in either the high or low resolution modes. As noted by Douglas, the slope of the side of the peak is largely determined by the mechanical quality of the rods employed (2,3). The particular rods used for these experiments were designed originally for GC-MS over a wide m/z range (up to m/z =1000). They were not built to have particularly high abundance sensitivity. When the

peaks are "squeezed" in the high resolution mode, use of a quadrupole with high abundance sensitivity should help exacerbate the loss of transmission at high resolution. Use of Stability Region III ($a \approx q \approx 3$) provides very high abundance sensitivity, as found by Douglas et al (3). Thus, it would be interesting to attempt to improve resolution by reflecting ions repetitively through a quadrupole operated in Region III, although it must also be noted that injecting ions is generally more difficult and less efficient when operating in alternate stability regions.

Conclusion

The results of this initial study show that the resolution from a quadrupole can be improved to at least 5000 (50% valley) by reflecting ions for multiple passes. The transmission decreases as resolution improves to a similar extent as that found using quadrupoles in alternate stability regions. Although a resolution of 5000 is not normally considered particularly "high" for most organic mass spectrometry, there are some applications that could be addressed already by this technique, such as resolution of polyatomic ions from atomic analyte ions in ICP-MS.

These experiments were done with an existing device to test the merit of the concept. Incorporation of ion optics specifically designed to reflect ions efficiently for only a fixed number of cycles should lead to additional improvements in resolution and a less severe compromise between resolution and transmission. Other refinements that may prove advisable include a) storing ions from the source, b) shutting the beam off so that no new ions are injected while one packet of ions is reflected, and c) tailoring the shape of the ion

packet during each reflection so that it matches the acceptance of the quadrupole. We also need to determine the basic causes of the shift in m/z scale and the satellite peaks.

It should be possible to implement these improvements without making the basic quadrupole mass analyzer much bigger or more expensive, which opens up possibilities for small, inexpensive mass spectrometers capable of moderate to high mass resolution. Such experiments are underway in our laboratory. The concepts described in this paper could also be valuable for improving the performance of the miniature quadrupole array mass spectrometers described recently (23).

Acknowledgements

This work was supported by the Laboratory Directed Research & Development Program of the Ames Laboratory, U. S. Department of Energy, Iowa State University. The mass spectrometer was donated by Roy L. M. Dobson of the Proctor & Gamble Company. Funds for the data system were provided by the Kresge Foundation. Harold Skank of the Ames Laboratory Electronics Shop designed the dual output voltage amplifier. Helpful comments from Don J. Douglas, Claude Beaugrand, and Urs Steiner are gratefully acknowledged.

References

1. Dawson, P. H., Ed. Quadrupole Mass Spectrometry and Its Applications, Elsevier, Amsterdam, 1976, pp. 23, 96, 125 and 143.

2. Ying, J.-F.; Douglas, D. J. *Rapid Commun. Mass Spectrom.* 1996, *10*, 649.

3. Du, Z.; Olney, T. N.; Douglas, D. J. *J. Amer. Soc. Mass Spectrom.* 1997, *8*, 1230-1236.

4. von Zahn, U. *Z. Phys.* 1962, *168*, 129-142.

5. Batey, J. Durham Conf. on Plasma Source Mass Spectrometry, Durham, UK, September 1994.
6. The a and q values that allow ions through the rods come from the Mathieu Equations (ref. 1) for ion motion. In a given stability region, these values are fixed for ions of all m/z values. In the usual mode of operation, the mass spectrum is scanned by changing the DC and RF voltages so that ions of the desired m/z ratio have (a,q) values inside the tip of the stability region, which corresponds to stable trajectories through the rods.

7. Dawson, P. H.; Bingqi, Y. *Int. J. Mass Spectrom. Ion Processes* 1984, *56*, 41-50.

8. Titov, V. V. *J. Amer. Soc. Mass Spectrom.* 1998, *9*, 50, 70.

9. Pedder, R. E.; Schaeffer, R. A. 44th ASMS Conf. Mass Spectrom. Allied Topics, Portland OR, May 1996.

10. Konenkov, N. V.; Kratenko, V. I. *Int. J. Mass Spectrom. Ion Processes* 1991, *108*, 115.

11. de Maack, F.; Devant, G.; Lapetit, G.; Rolando, C. 36th ASMS Conf. On Mass Spectrom. Allied Topics, San Francisco, CA, Paper No. 817.

12. Beaugrand, C., personal communication, 1998.

13. Miteseki,K. U.S. Patent 5,227,629, July 1993.

14. Mamyrin, B. A.; Karataev, V. I.; Shmikk, D. I.; Zagulin, V. A. *Soviet Phys. JETP* 1973, *37*, 45.

15. Wollnik, H.; Przewloka, M. *Int. J. Mass Spectrom. Ion Processes* 1990, *96*, 267-274.

16. Benner, H. W. *Anal. Chem.* 1997, *69*, 4162.

17. Dolnikowski, G. G.; Kristo, M. J.; Enke, C. G.; Watson, J. T. *Int. J. Mass Spectrom. Ion Processes* 1988, *82*, 1-15.

18. Beaugrand, C.; Jaouen, D.; Mestadagh, H.; Rolando, C. *Anal. Chem.* 1989, *61*, 1447 - 1453.

19. Beaugrand, C.; Devant, G.; Jaouen, D.; Mestadagh, H.; Rolando, C. 35th ASMS Conf. on Mass Spectrom. Allied Topics, Denver, CO, May 1987, Paper No. 209 and 345; 36th ASMS Conf. on Mass Spectrom. Allied Topics, San Francisco, CA, May 1988, Paper No. 466 and 811.

20. Huang, Y.; Li, G.-Z.; Guan, S.; Marshall, A. G. *J. Amer. Soc. Mass Spectrom.* 1997, *8*, 962-969.

21. Steiner, U., personal communication, 1998.

22. Kaiser, R. E., Jr.; Cooks, R. G.; Stafford, G. C., Jr.; Syka, S. E. P.; Hemberger, P. H. *Int. J. Mass Spectrom. Ion Processes* 1991, *106*, 79; Williams, J. D.; Cox, K. A.; Cooks, R. G.; Kaiser, R. E., Jr.; Schwartz, J. C. *Rapid Comm. Mass Spectrom.* 1991, *5*, 327.

23. Ferran, R. J.; Boumselk, S. *J. Vac. Sci Technol.* 1996, *A14*, 1258-1265; Orient, O. J.; Chutjian, A.; Garkanian, V. *Rev. Sci. Instrum.* 1997, *68*, 1393-1397.

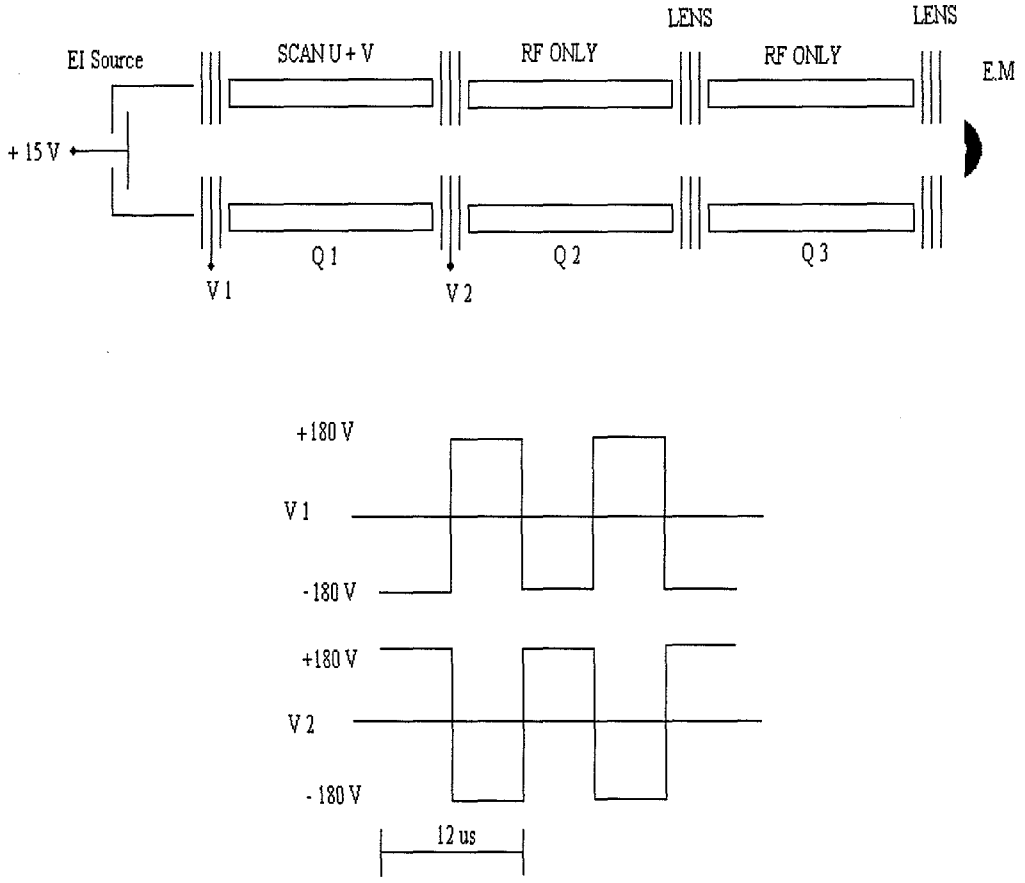

Fig. 1. Apparatus for reflecting ions through a quadrupole MS. Square wave voltages of opposite sign are applied to the lenses V_1 and V_2 as shown. The delay time and amplitude are adjusted empirically to optimize the resolution for the m/z value of the ion monitored; 12 μs and ±180 volts are typical for the ions measured in this paper.

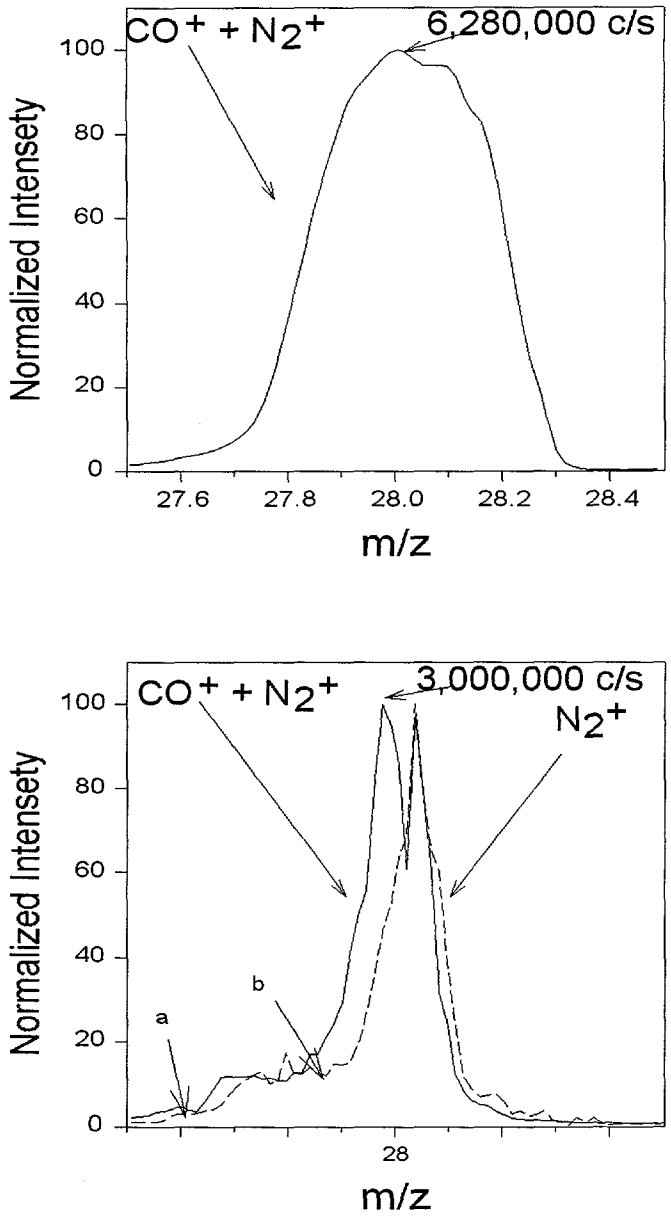

Figure 2. Low resolution scan (top) compared to high resolution scan (bottom) of ions being reflected through a quadrupole MS. The conventional resolution setting (i.e., the ratio of DC/RF voltages applied to the rods) is the same in both spectra. The CO^+ peak disappears when CO is removed from the ion source. Note also the plateau between points a and b on the low-mass side of the high resolution peak.

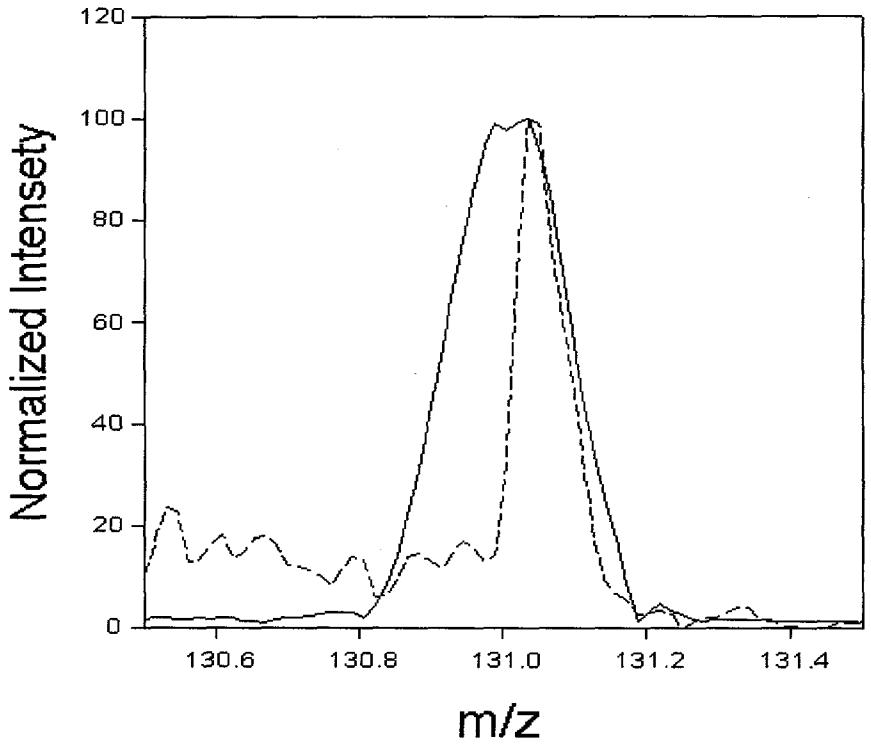

Fig. 3. Scans of $C_3F_5^+$ (m/z = 131) and $C_4F_9^+$ (m/z = 219) at low resolution (solid line) and high resolution (dotted line). The high resolution peaks have been shifted back underneath the low resolution ones. The peak heights have been normalized; the intensities of the high resolution peaks are about 30% of that of the low resolution ones.

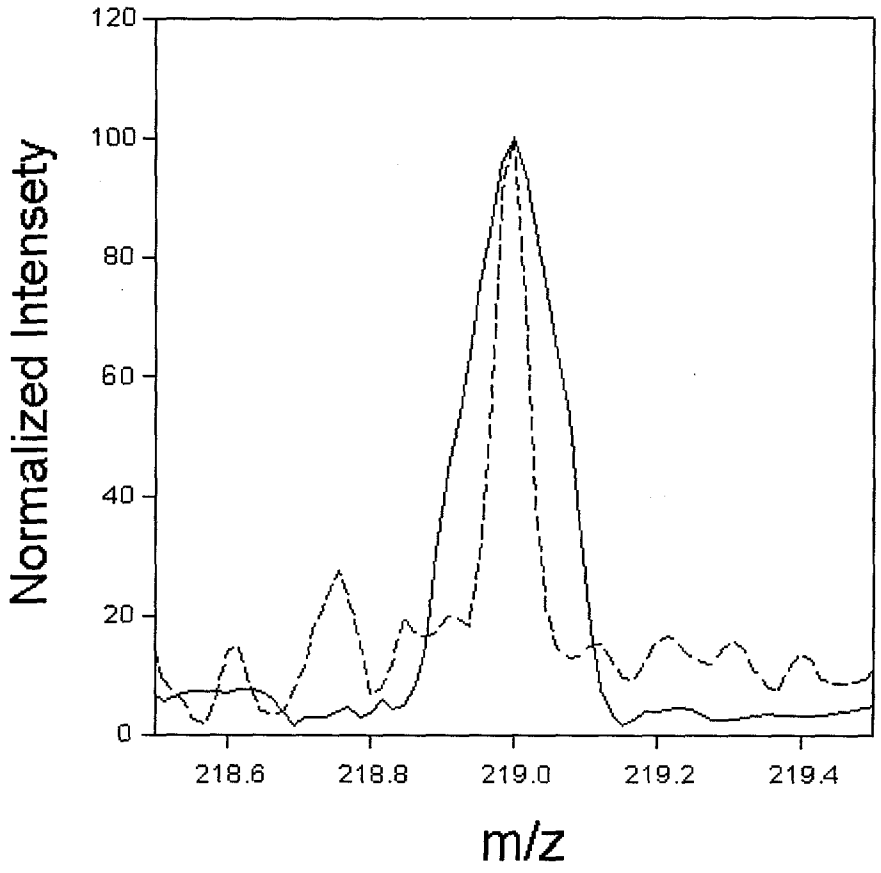

Figure 3. Cont.

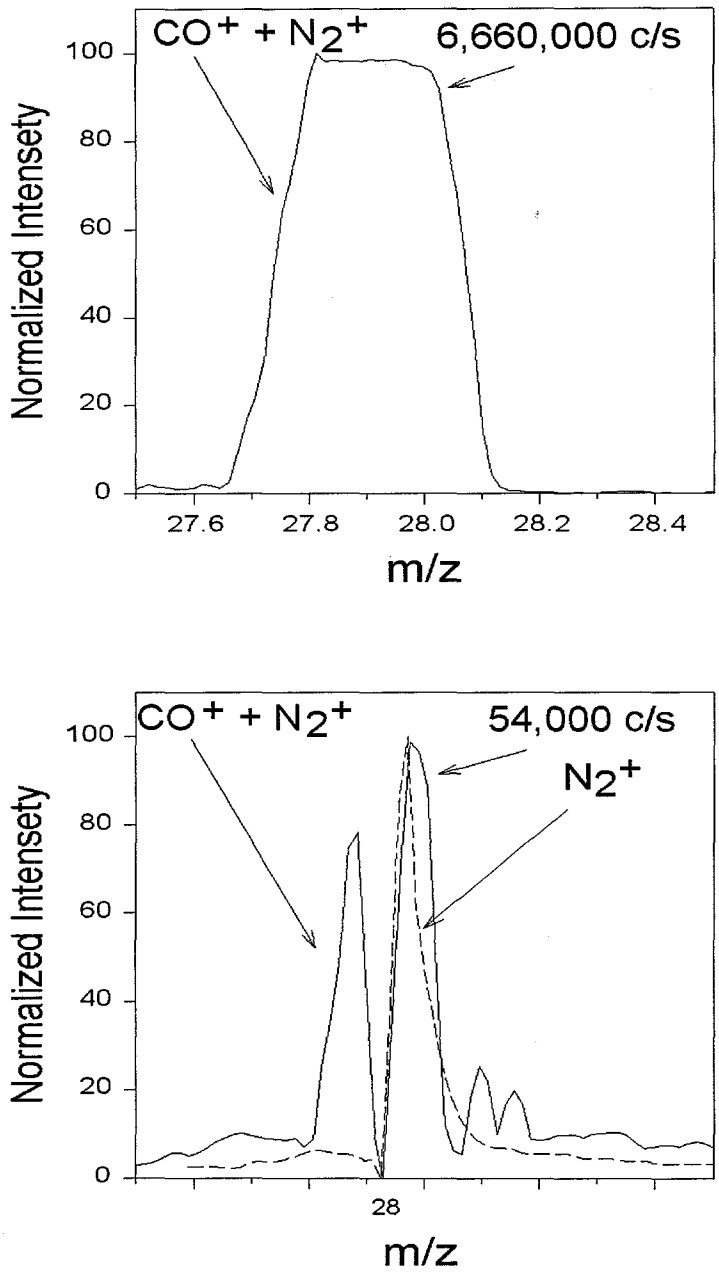

Fig. 4. Low (top) and high resolution spectra (bottom) with grid ion lenses. CO^+ and N_2^+ are resolved to baseline in the high-resolution spectrum, but at a substantial sacrifice of sensitivity.

CHAPTER 4. MASS RESOLUTION OF 22,000 WITH 63% OF THE ORIGINAL SIGNAL REMAINING WITH A MULTIPLE PASS QUADRUPOLE MASS ANALYZER

A paper to be submitted to the Journal of the American Society for Mass Spectrometry

Ma'an H. Amad and R. S. Houk

Abstract

CO^+ and N_2^+ have been separated with a conventional quadrupole mass spectrometer by using a multiple pass quadrupole mass analyzer. A resolution of 22,000 (FWHM) with 63 % of the total signal remaining was attained. A gated ion extraction method was employed to inject ions into the multiple pass quadrupole mass analyzer in bursts of about 10 μs duration. The gated ion extraction was found to reduce the severity of artifact peaks observed when the ions are injected continuously.

Introduction

The quadrupole mass analyzer has become one of several standard instruments for chemical analysis, environmental monitoring and residual gas analysis (1-6). These devices are generally operated in the first stability region and are generally limited to unit mass resolution. As is well known in a conventional quadrupole mass analyzer, a combination of a dc (U) and an rf (Vcos ωt) voltage are applied to the quadrupole electrodes. When an ion of mass m and charge z enters the hyperbolic field, it will wobble inside the rods under the influence of the combined DC and oscillating RF field. As ions drift inside the poles along

the z axis, their stable motion in the x-y plane is expressed in terms of the Mathieu equations, which will be represented by

$$d^2X/d\zeta^2 + (a + q \cos 2\zeta)x = 0$$

$$d^2y/d\zeta^2 - (a + q \cos 2\zeta)y = 0$$

and

$$a_x = -a_y = 4eU/m\omega^2 r_o^2$$

$$q_x = -q_y = 2eV/m\omega^2 r_o^2$$

where r_o is the radius from the center axis to the rod, ω is the angular frequency and $\zeta = \omega t/2$. If the applied electrical potential within the rods ϕ_o is constant there will be a simple harmonic motion in the xz plane for any ion injected into the quadrupole and all ion trajectories would be stable. This condition for ion stability is expressed and explained in what is known by the stability diagram (7).

Different researchers have obtained high resolution in a quadrupole mass analyzer by using alternative stability regions (8). Dawson and Binqi (9) were first to study the second stability region and resolved $^{131}Xe^+$ from $C_3F_5^+$ ions at a kinetic energy of 300 eV. Douglas and coworkers (10) utilized this stability region to resolve $^{56}Fe^+$ from $^{40}Ar^{16}O^+$ interference in inductively coupled plasma mass spectrometry. Other workers utilized other stability zones such as the third stability region to obtain high resolution (11-13).

Another way to obtain high resolution in a quadrupole was demonstrated by de Maack et al (14), Mitseki (15) and Beaugrand (16) who applied an additional sine wave to the rods of the analyzer. This sine wave was found to narrow the range of m/z values associated with the stable trajectories and thus improve the resolving performance of the quadrupole without changing the U/V ratio applied to the rods.

The main limitation on resolution of a quadrupole mass analyzer is the separation time (17), which is mainly characterized by the number of rf cycle an ion spends inside the rods. The maximum resolution R is roughly proportional to the square of the number of RF cycles by the following proportionality

$$R \alpha n^2 \alpha m f^2 L^2 / zV_z$$

where n is the number of RF cycles, f = frequency of RF voltage applied to the rods, L = length of rods, z = ion charge and V_z = potential drop between source and mass analyzer, i.e., zV_z is the ion kinetic energy inside the mass analyzer.

Several workers have achieved high resolution in a quadrupole mass analyzer by a) increasing the electrode length (L)(18), b) increasing the frequency (f) (19), and c) decreasing the kinetic energy of the ions (V_z)(20). Since resolution is proportional to n^2, we showed in our earlier work the feasibility of obtaining high resolution by reflecting or trapping the ions inside a quadrupole (21). Improvement in resolution also seen in quadrupole ion trap; Cooks and coworkers obtained high resolution in the ion trap by scanning the ions out slowly so that they stay inside the trap for a longer time (22). Enke and coworkers (23) pulsed the ion lens in front of an rf-only quadrupole collision cell to increase the ions opportunity for ion-molecular reaction. Douglas and coworkers (24) used a pulsed

lens to gate the ions in front of a two dimensional ion trap. Marshall and coworkers (25) employed a linear ion trap for Fourier transform ion cyclotron resonance MS in which ions are reflected back and forth through a quadrupole structure inside an axial magnetic field.

In a regular arrangement, an electron impact source operates continuously and ions are also extracted and injected into the quadrupole continuously. Wollnik and coworkers (26) used a pulsed storage ion source that produce ions continuously, stored them and released them in bursts of 10 μs duration. In the present work, we pulsed and gated the voltage applied to ion extractor lens in front of the electron impact source so that a finite batch of ions is extracted from the source and then injected into the quadrupole. This gated ion extraction reduces the severity of stray "artifact" peaks observed when the ions are injected continuously. A resolution of 22,000 with 63 % of the original signal remaining was obtained in this experiment by a repetitive trapping of ions inside the quadrupole mass analyzer while injecting finite batches of ions into the quadrupole.

Experimental Section

The instrument, described in detail elsewhere (21), is a triple quadrupole mass analyzer (Finnigan MAT TSQ 4500) with quadrupole two and three in rf only mode (Figure 1).

Ions are produced by an electron impact source with 70 eV electrons and a repeller voltage of + 15 V. In a regular resolution mode (single pass) the triple quadrupole was operated in the traditional single pass mode. In a high resolution mode (multiple pass) a square wave voltage of ~ 100 V p-p and a frequency of ~ 50 kHz (period 20 μs) was applied to the entrance and exit lenses of the first quadrupole (V1 and V2). In this mode, ions formed

at the source are injected into Q1 when V1 is – 50 V. Within the timing sequence of 20 μs these ions travel through Q1 (i.e, from left to right in Fig. 1) until they are reflected by the +50 volts on V2. These reflected ions will travel backwards (from right to left) in Q1 toward the source and be reflected in the original direction to Q1 by the +50 volts applied on to V1. This batch of ions will travel back through Q1 towards V2, Eventually some of the ions escape through V2 into Q2, pass through Q3 and then strike the detector.

In a gated ion extraction high resolution multiple pass mode (GIE-HRMP) the ions are stored in the source by applying a slightly positive potential to the extractor lens (L1) with respect to the repeller voltage (see figure 1). In principle the ions produced in the source can be accelerated toward and through the aperture L1 (continuous mode). To store the ions for a certain time a positive potential of +30 V is applied for 100 μs. This applied potential on L1 will trap and store the ions inside the source unless their kinetic energy is larger than the lens potential or until the ions are extracted by applying a negative potential of - 30 V for 10 μs.

At first the resolution of the mass analyzer was roughly adjusted to obtain a low resolution spectrum with usual negative dc voltages on the ion lenses. The conventional resolution setting was not changed further. Once the mass range is calibrated, the reflecting voltages are applied on V1 and V2 to obtain the high resolution spectrum while adjusting the frequency and amplitude of the square wave output from the function generator. This was done manually to produce the desired resolution. Once a high resolution spectrum is obtained, the voltage applied to L1 is also pulsed as shown in Fig. 1. The timing diagram at

the bottom of figure 1 illustrates the reflecting function of lenses V1, V2 and the gated ion storage source lens L1.

Samples Gases were obtained from Air Products .The calibration compound perfluorotributylamine (CF43) was obtained from Scientific Instrument Services. The samples were introduced into the source by a gas inlet line.

Results and Discussion

Results with continuous ion extraction Presented in this section are representative mass spectra taken with a multiple pass mode quadrupole mass analyzer with a continuous electron impact source.

All spectra were taken with the optimum mass resolution and at fixed electron energy of 70 eV. Shown in Figure 2 are mass spectra of air taken at both modes of operation. Some significant peak plateau and artifact peaks are obvious in front of the O_2^+ peak in the high resolution mode. The artifact peaks are described in detail later. The nominal value of m/Δm improves to 1500 (50 % valley) at m/z 32. The peak height at high resolution is ~ 5% of that at low resolution. The air spectrum in Figure 2 has more O_2^+ than N_2^+ due to the confined space of the source that leads to ion-moleculer and charge transfer reactions of O_2^+ to form NO^+ and more N_2^+.

In order to test the analyzer at higher mass range, a sample of perfluorotributylamine was analyzed. Mass spectra of ions such as CF_3^+ and $C_4F_9^+$ from perfluorotributylamine are shown in figure 3. In multiple pass mode, the nominal value of m/Δm improves to 6600 (50%

valley) at m/z 219 and 2100 (50% valley) at m/z 69. At m/z 219 and 69 the peak heights at high resolution are ~ 20% and ~ 8% of that at low resolution. The background at high resolution is due to noise from the data acquisition system not from the reflection technique. The reflecting operation frequency in high resolution mode was selected to be ~ 20 μs. The voltage on the grid lens (45 mesh lines / cm wire diameter 0.28 mm) was approximately 70 V.

Results are shown in Figure 4 for a mixture of N_2 and CO with a 20 eV kinetic energy. In these experiments there is a peak shift to a higher apparent mass value. This mass shift was found to be approximately one mass unit. Calibration of mass scale is necessary with any quadrupole. The results shown here are shifted back to the original known m/z. Some significant peak plateau is obvious in front of the CO^+ peak at a high resolution spectra (bottom spectra) as shown in figure 4. This peak plateau is less severe than that observed in the initial studies.

Figure 4 shows that few stray peaks are observed in the mass spectra if the scan window is narrow (one mass unit). Meanwhile stray peaks are much more severe if the scan window is more than one mass unit and if several ions at different m/z value are present in the source (Figure 2). Figure 2 shows the satellite peaks in front of the O_2^+ peak of the mass spectra. The presence of these satellite peaks are thought to be due to ions at m/z 32 that either getting out after only one pass or 3 passes. To reduce the artifact peaks experiments were performed by pulsing and gating the extractor lens L1 in front of the ion source so that only one finite batch of ions is reflected in the quadrupole.

In terms of sensitivity the initial results ~ 80 –90 % loss of signal in multiple pass mode. This compromise in sensitivity is similar to that usually observed with alternative stability regions and magnetic sector. In addition peak shape was observed to be more symmetric than that previously obtained (21). In this work we showed that a resolution of 11,000 was obtained for an ions with kinetic energy of 20 eV. This was done by applying a pole bias to the quadrupole. This pole bias will slow down the ions inside the rods and thus increase their duration inside the quadrupole.

Results with gated ion extraction This set of experiment was performed to determine the effect of pulsed introduction of ions on the multiple pass quadrupole mass analyzer and determine the detection efficiencies of ions of different mass. The spectra are shown in Figures 5 , 6, 7 and 8. To resolve a mixture, CO and N_2 were introduced into the gated source. Figure 5 shows the mass spectra at both high and low resolution mode. Most of the plateau and the satellite peaks are indeed removed, and CO^+ (m/z = 27.99437) separated from N_2^+ (m/z= 28.0056). In the high resolution spectrum, the CO^+ peak disappears when CO is removed from the source (dotted line). The numerical value of $m/\Delta m$ improves to 22,000 (50% valley) with 63% of the original signal remaining.

Figure 6, the solid line, shows the mass spectrum of Kr in multiple pass mode. Here the reflecting voltages V1 and V2 were 100 V p-p. The voltage on the grid lenses was approximately –30V. Only a finite ion batch with duration of 20 μs was injected into the multiple pass quadrupole mass analyzer. A numerical value of resolution $m/\Delta m \sim 1200$

(50 % valley) is obtained while scanning for a wider mass range (80-87 m/z). An improvement in resolution is obtained if the system was used within a one unit mass scan (m/Δm 50 % valley ~ 2000 at m/z 84).

In multiple pass mode, the ion signal for all Kr ions with gated ion extraction increased significantly compared to that obtained with continuous ion extraction. The peak heights in the high resolution mode are almost one third of those in the low resolution mode. This spectrum at high resolution still resembles that of Kr. Some artifact peaks are displayed in the spectrum. The artifact peaks are shown by asterisks. The shift of m/z position was less sever than that observed with continuous ion extraction. The slopes of the back sides of the Kr peaks in high resolution mode resembled the slopes in the low resolution mode. As mentioned by Douglas and co-workers, the peak shape of the quadrupole is largely dependent on the mechanical quality of the rods used.

Figure 7 shows the mass spectra of CF_3^+ and $C_3F_5^+$ from perfluorotributylamine. In a multiple pass mode, a numerical value of resolution (m/Δm ~ 50% valley) ~ 1200 at m/z 69 and ~ 1900 at m/z 131. The peak height at m/z 69 at low resolution is actually ~ 20 % more of that at low resolution, meanwhile ~ 35% less at m/z 131. An improvement in resolution at m/z 69 and 131 were also obtained with a moderate sacrifice in sensitivity. An improvement in resolution from 1200 to 1700 at m/z 69 with 6 % of signal remaining, meanwhile a 2 fold increase in resolution at m/z 131 (from 1900 to 3500) with 50 % of signal remaining is observed. An artifact peak "satellite" is observed as a shoulder peak on the tail of the high resolution peak at m/z 69 and 131. It should be noted than when the quadrupole was operated

in a low resolution "single pass" with a gated ion extraction, a slight increase in ion signal was observed.

Artifact peaks and mass shift When ions are analyzed using the multiple pass high resolution mode, additional poorly reproducible peaks often appear in the spectra. These artifacts are shown by asterisks in the various figures. Careful analysis of the spectra in high resolution mode indicates that these artifacts are identified into two types. a) Satellites peaks close to the main peak. These satellites are usually seen. b) Other distant artifacts from the main peak. These artifacts are less common and less reproducible. In all these spectra, the formation of these artifacts cannot be explained by simple fragmentation reactions of the parent ions or by the isotopic pattern.

The spectra obtained with gated ion extraction arrangement have fewer artifact peaks than those obtained with continuous ion extraction. The gated ion extraction seems to reduce the artifact peaks by injecting ions only in a discrete 10 μs bunch into the quadrupole. In addition, with gated ion injection the mass shift was less severe. Cooks reported variations in peak position in quadrupole ion trap mass spectrometry based on the total number of ions inside the trap (27). This shift was explained by local space charge between ions of the same m/z value and by ion-ion interaction between species separated by large mass difference.

A comparison of the area of total ions of both spectra displayed in Figure 8 shows the relationship of the severity of artifacts as a function of resolution and transmission. From these, it can be seen that as the area of the total ions injected in the quadrupole increases (Figure 8b), the artifact peaks become numerous and more intense. Apparently, the number and abundance of artifact peaks become worse as more ions are trapped inside the

quadrupole. Tabet and coworkers observed a similar trend of signal and resolution loss in their study of "ghost peaks" in ion trap mass spectrometry. Such ghost peaks are largely dependent upon space charge produced during the injection step (28). Todd and coworkers reported the presence of ghost peaks caused by non-linear fields in the quadrupole ion trap (29). The formation of these ghost peaks occurs when a portion of a given m/z ion population is prematurely ejected at one of the nonlinear resonance lines. This gives rise to an ion signal not only from an ion population at the correct m/z in the spectrum, but additionally at a lower m/z value. These non-linear resonance ghost peaks disappeared at a particular cut-off pressure of the buffer gas. A similar observation of the presence of anomalous mass peaks at a lower mass value than the actual m/z was reported by Wells and coworkers (30).

Each ion of particular m/z has a unique fundamental resonant frequency given by (7,24)

$$\omega_0 = \beta\omega/2 \sim q_u\, \omega/(8)^{0.5}$$

where ω is the angular frequency, q_u is the Mathieu parameters and β is a parameter characterizing the nature of ion motion in the stable region which is proportional to q_u.

The appearance of artifact peaks in the spectra of figure 8b and a decrease in resolving power can be explained as following. A space charge condition is analogous to adding a slight DC potential to the rods and therefore moves the resonance point to a higher q value. Since R is proportional to 1/q , a higher q value will decrease the resolution. Since m/z is proportional to 1/q , an increase in q value can produce an artifact peak at lower m/z value in the spectrum.

Conclusion

These studies confirm and improve upon our preliminary results that reflecting the ions inside the quadrupole can indeed increase the resolution of a quadrupole. With lower voltages applied to the reflecting lens we were able to reflect the ions closer to the quadrupole. Indeed with this set of reflecting conditions and the usage of a continuous ion extraction lens, we were able to improve the resolution by two fold (resolution of 11,000) and improve the transmission by 8 fold compared to the previous results. In this experimental set up there is a peak shift to a higher apparent mass value.

When a gated ion extraction lens is used, a resolution of at least 22,000 can be achieved. The gated ion extraction was found to reduce, but not eliminate, artifact peaks and peak shifts observed when the ions are injected continuously. In general, the artifacts and mass shift decrease with increasing mass differences between the ions of interest and neighboring ions and increasing with increasing abundances of surrounding ions. Overall, these observation are similar to the trend observed in ion traps. Current work in our lab undergoes in using this technique to resolve the problem of polyatomic ion interferences in ICP-MS. Furthermore work on basic modeling the reflected ion beam with modeling programs is needed to understand the trapping process.

Acknowledgment

Ames Laboratory is operated by Iowa State University for the U. S. Department of Energy under Contract No.W-7405-ENG-82. This work was supported by the LDRD program at DOE, Iowa State University. The authors thank Dow Chemical Company for

their funding through a graduate fellowship. Proctor and Gamble donated the mass spectrometer.

References

1. White, F.A.and G.M. Wood, *Mass Spectrometry: Applications in Science and Engineering*. New York: Wiley-Interscience, 1986.

2. Watson, J.T., *Introduction to Mass Spectrometry*, New York: Raven Press, 1985.

3. Duckworth, H.E., Barber,R.C., and V.S. Venkatasubramanian, *Mass Spectroscopy*, 2nd ed. Cambridge, U.K.; Cambridge University Press, 1986.

4. Ross, M.E. and Johnstone, A.W. *Mass Spectrometry for Chemists and Biochemists*. New York: Cambridge University Press, 1982.

5. Eadon,G.A., in *Treatise on Analytical Chemistry*, 2nd ed.

6. Houk, R.S., Fassel, V.A., Flesch, G.D., Svec, H.J., Gray,A.L. and Taylor, C.E., *Anal. Chem.*, 1980,**52**,2283.

7. Dawson, P.H., Ed. *Quadrupole Mass Spectrometry and Its Applications*:Elsevier: Amsterdam,1976.

8. Du,Z. Douglas,D.J.; Konenkov,N.V., *J. Anal. Atom. Spectrom.* In press, 1999.

9. Dawson, P.H., and Bingoi,Y, *Int. J. Mass Spectrom, Ion processes*, 1984,**56**,25.

10. Ying, J.F., Douglas, D.J. *Rapid Commun. Mass Spectrom.* 1996,**10**,649.

11. Konenkov,N.V.: Mogilchenko,S.A.; Silakov,S.S.; Shagimuratov,G.I. *Sovi J. Tech. Phys.* 1990,**60**,148.

12. Konenkov,N.V; Kratenko,V.I. *Int. J. Mass Spectrom. Ion proc*, 1991,**108**,115.

13. Dawson, P.H. *J. Vac. Sci. Technol.* 1974, **11**, 1151-1153.

14. de Maack, F.; Devant, G.; Lapetit, G.; Rolando, C. 36th ASMS Conf. On Mass Spectrom. Allied Topics, San Francisco, CA, Paper No. 817.

15. Miteki, K. U.S.Patent 5,227,629, July 1993.

16. Beaugrand, C. Personal comunication, 1998.

17. Titov, V.V. *J.Am. Soc. Mass Spectrom.* 1998,**9**,50,70.

18. Von Zahn,U.*Z. Phys.* 1962,**168**,129-142.

19. Batey, J. Durham Con. On Plasma mass Spectrometry, Durham UK, September 1994.

20. K. Willmaaek. *Vacuum*, 326, **1982**,65.

21. Amad,M.H.: Houk, R.S, *Anal. Chem.*, 1998, **70**, 4885-4889.

22. Kaiser, R. E., Jr.; Cooks, R. G.; Stafford, G. C., Jr.; Syka, S. E. P.; Hemberger, P. H. *Int. J. Mass Spectrom. Ion Processes* 1991, *106*, 79; Williams, J. D.; Cox, K. A.; Cooks, R. G.; Kaiser, R. E., Jr.; Schwartz, J. C. *Rapid Comm. Mass Spectrom.* 1991, *5*, 327.

23. Dolnikowski, G. G.; Kristo, M. J.; Enke, C. G.; Watson, J. T. *Int. J. Mass Spectrom. Ion Processes* 1988, **82**, 1-15.

24. Campbell, J.M., Collings, B.A., and Douuglas, D.J. *Rapid Commun. Mass Spectrom.* 1998, **12**, 1463.

25. Huang, Y.; Li, G.-Z.; Guan, S.; Marshall, A. G. *J. Amer. Soc. Mass Spectrom.* 1997, *8*, 962-969.

26. Grix, R., Gruner,U.,Li,G.,Strolt,H. and Wollnik,H. *Int. J. Mass Spectrom. Ion Proc.*, 1989, **9**,323.

27. Cox, K.A.,Cleven, C.D. and Cooks, R.G. *Int. J. Mass Spectrom. Ion Proc.*, 1995, **144**,47.

28. Kocker,K. Favre, A., Gonnet, F. and Tabet, J.C., *Journal of Mass Spectrometry*, 1998, **33**, 921.

29. Mo, W., Langford,M.L. and Todd, J.F, *Rapid Comm. Mass Spectrom.,* 1995,**9**,107.

30. Lammert,S.A and Wells, J.M. , *Rapid Comm. Mass Spectrom.,* 1996,**10**,361.

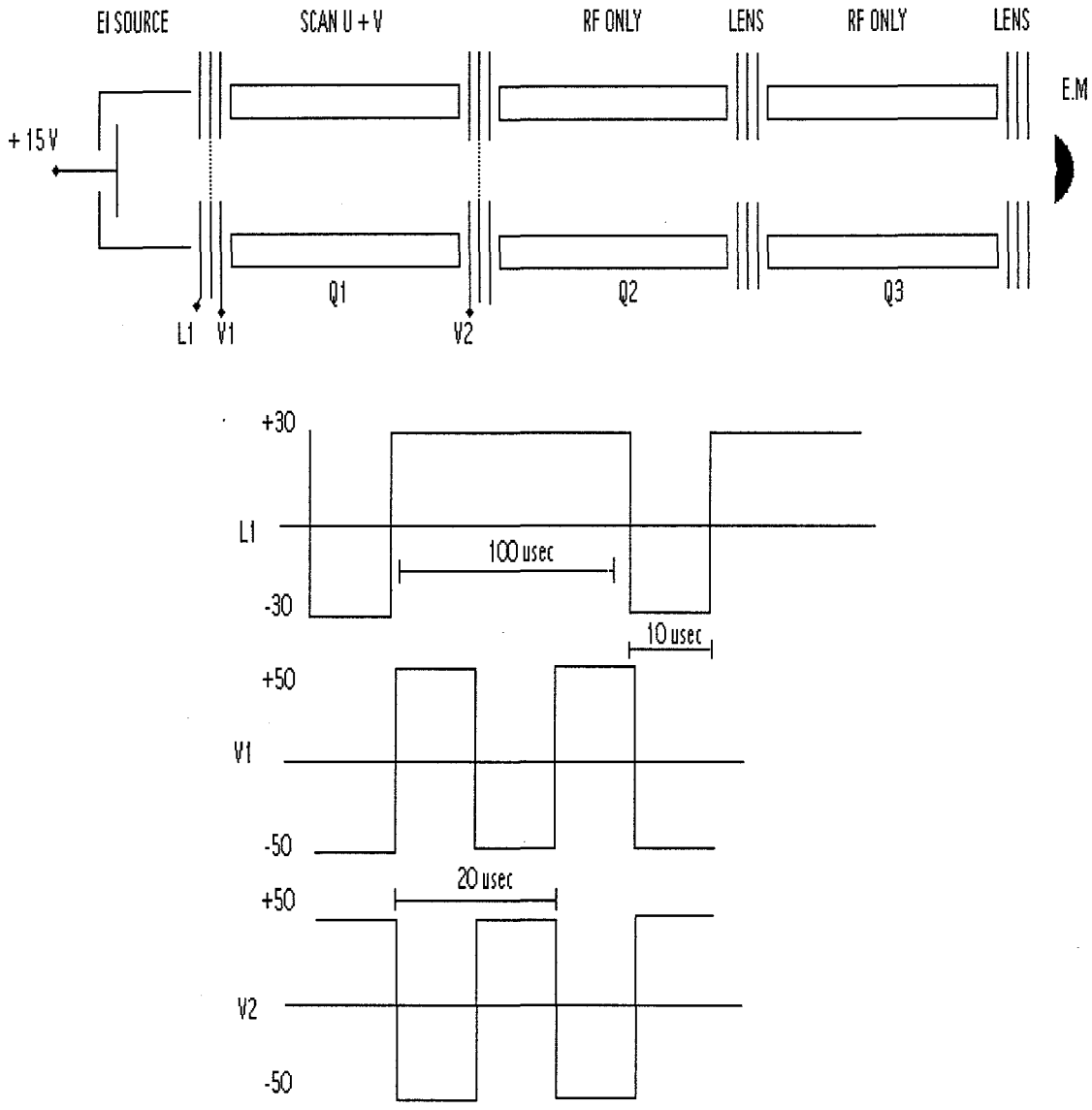

Figure 1. Apparatus for reflecting ions through a quadrupole mass analyzer.

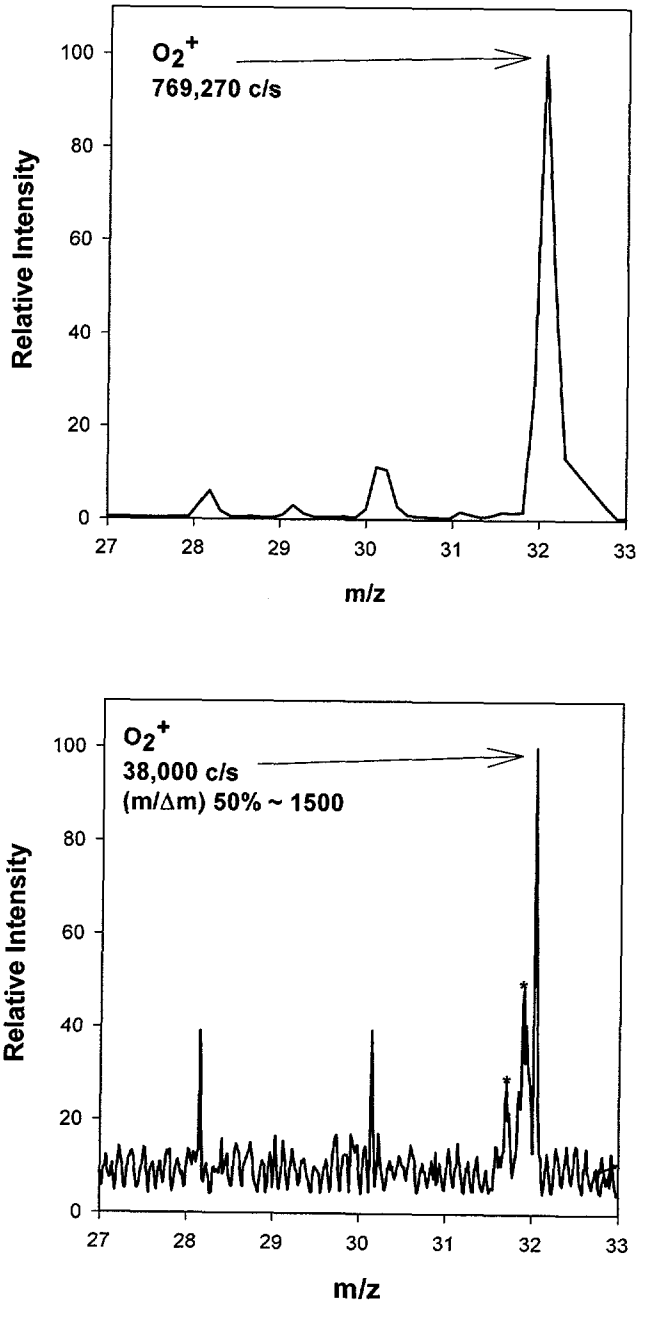

Figure 2. Low (top) and high resolution spectra (bottom) for air with non gated ion extraction. The peak heights have been normalized.

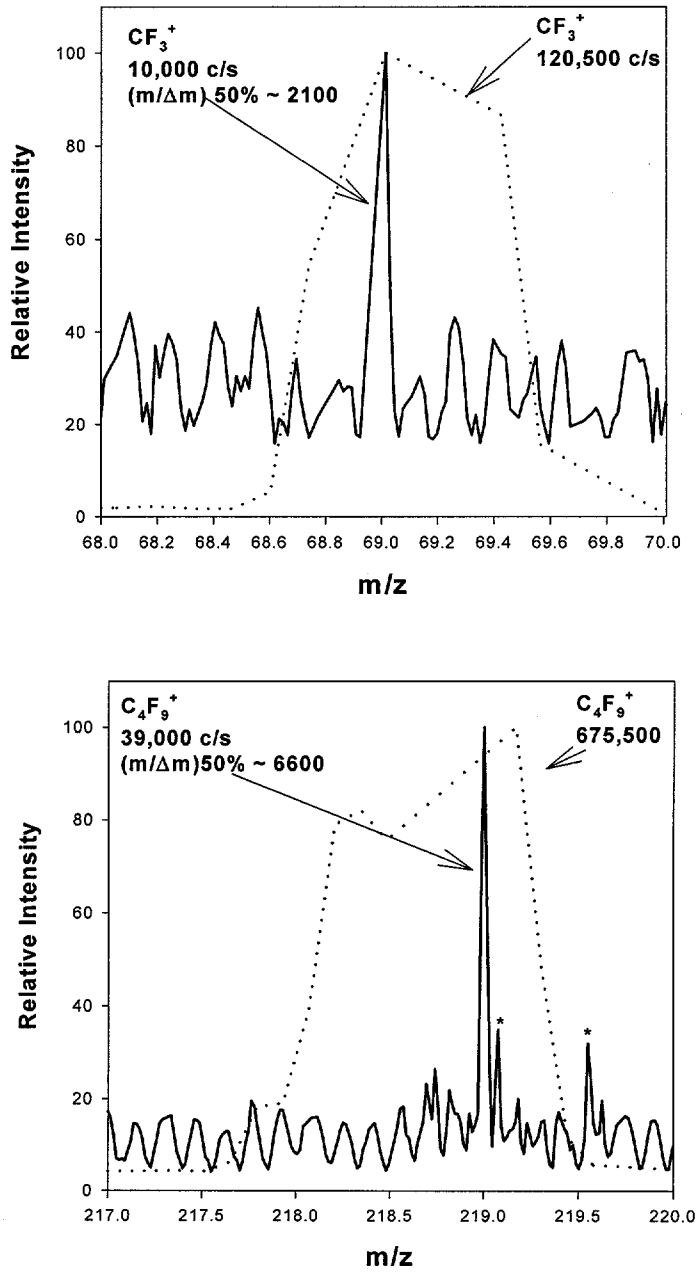

Figure 3. Scans of CF_3^+ (m/z = 69) and $C_4F_9^+$ (m/z 219) at low resolution (dotted line) and high resolution (solid line) with non gated ion extraction.

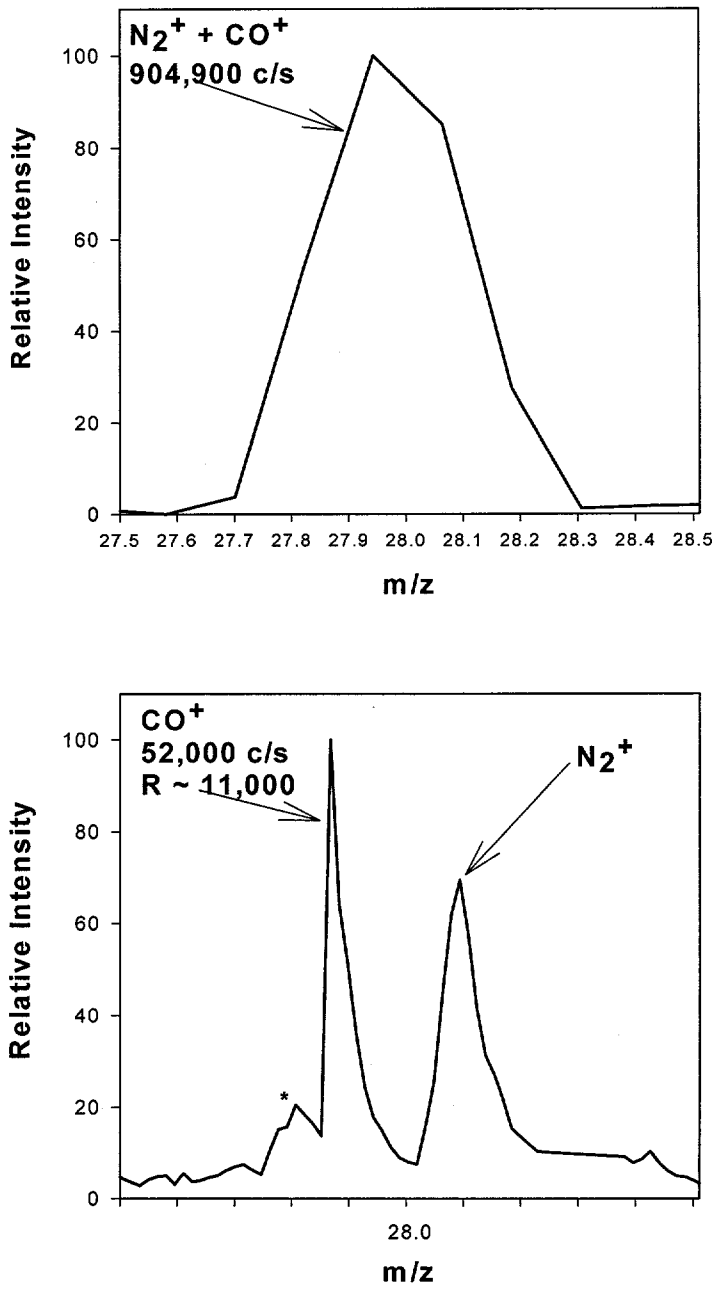

Figure 4. Low (top) and high resolution spectra (bottom) with non gated ion extraction. CO^+ and N_2^+ are resolved with a resolution of 11,00 at base line.

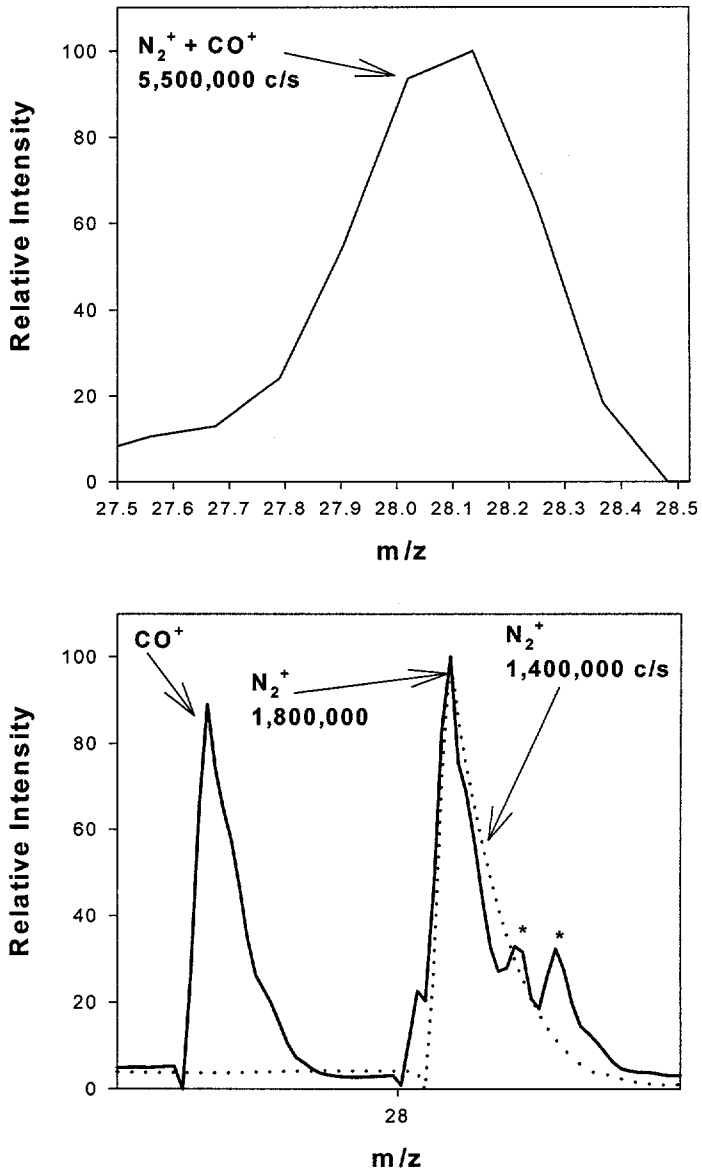

Figure 5. Low (top) and high resolution spectra (bottom) with gated ion extraction. CO^+ and N_2^+ are resolved with a resolution of 22,00 at base line. The dotted line is N_2^+Only.

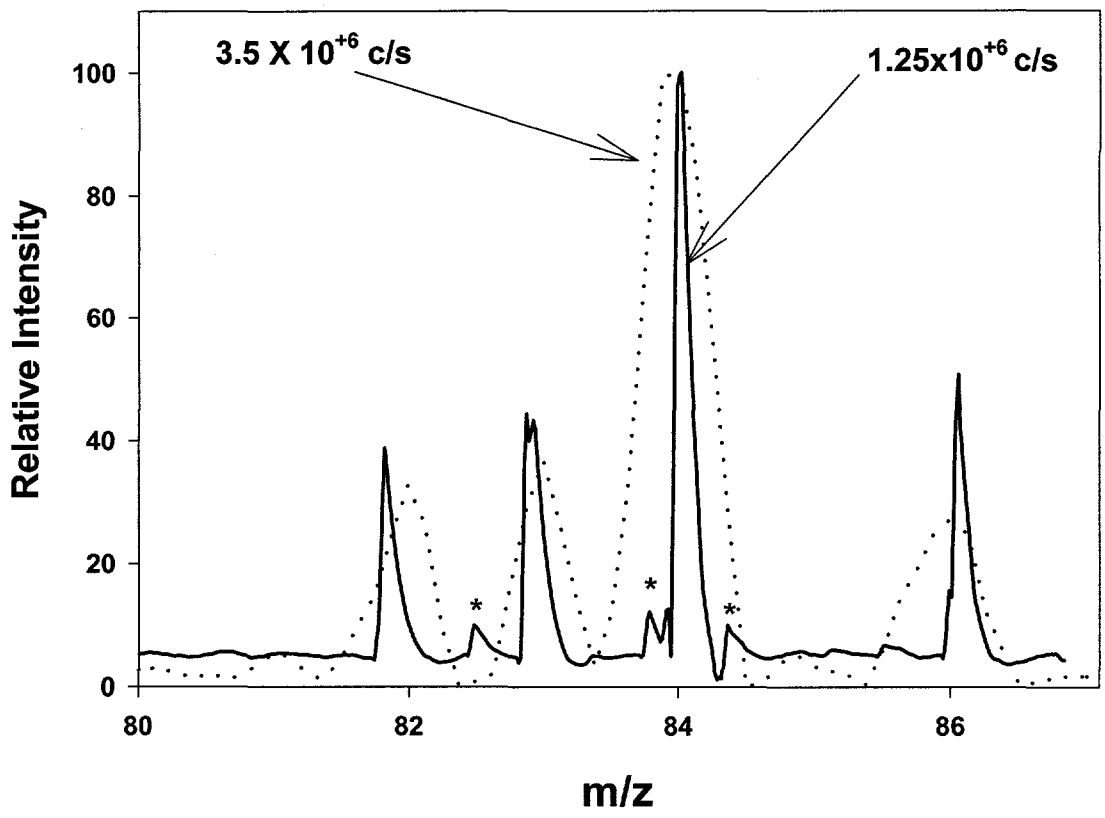

Figure 6. Scans of Kr^+ isotopes at high resolution (solid line) and low resolution (dotted line) with gated ion extraction.. The peak heights have been normalized, the intensity of the high resolution spectrum is 33% of that of the low resolution one.

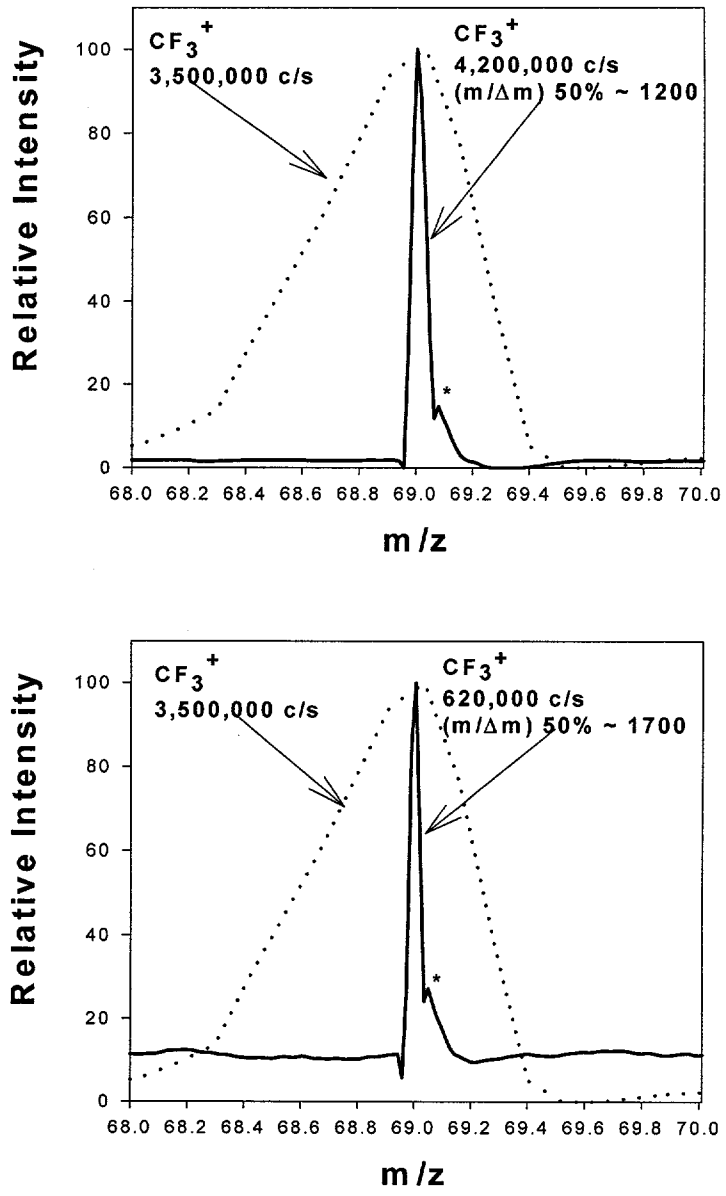

Figure 7a. Scans of CF_3^+ (m/z = 69) at low resolution (dotted line) and high resolution (solid line) with gated ion extraction.

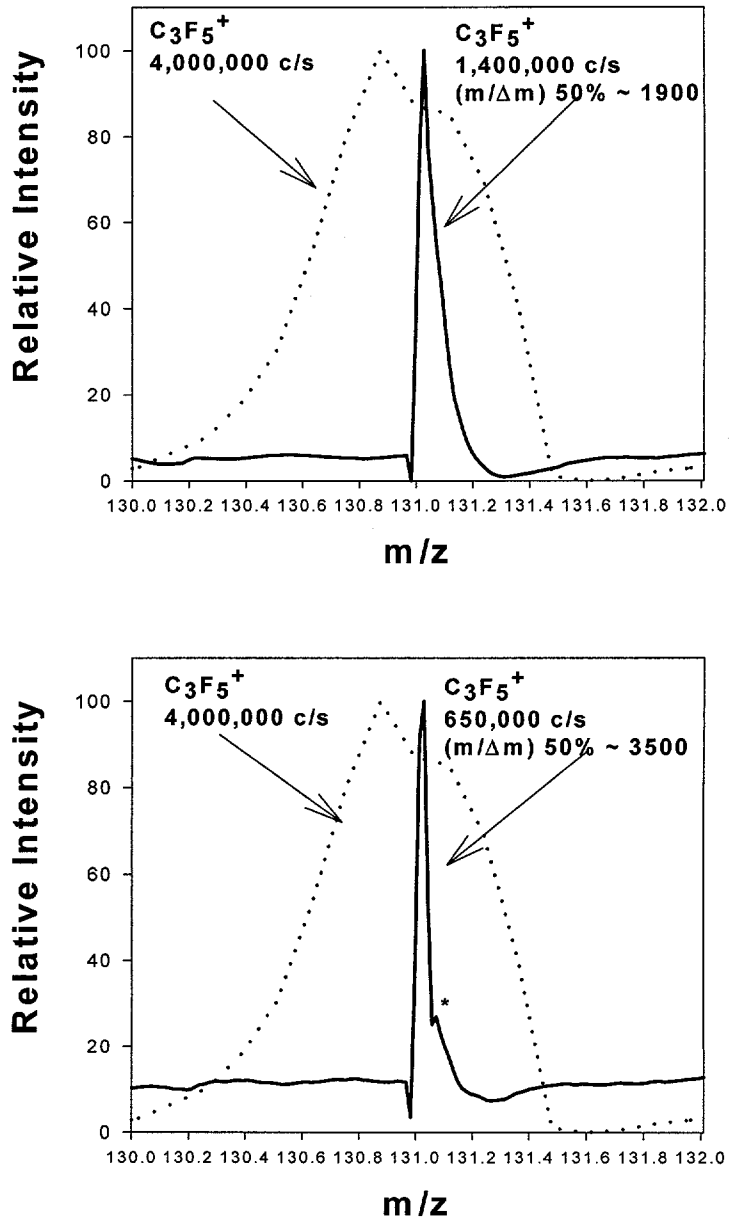

Figure 7b. Scans of $C_3F_5^+$ (m/z = 131) at low resolution (dotted line) and high resolution (solid line) with gated ion extraction.

a)

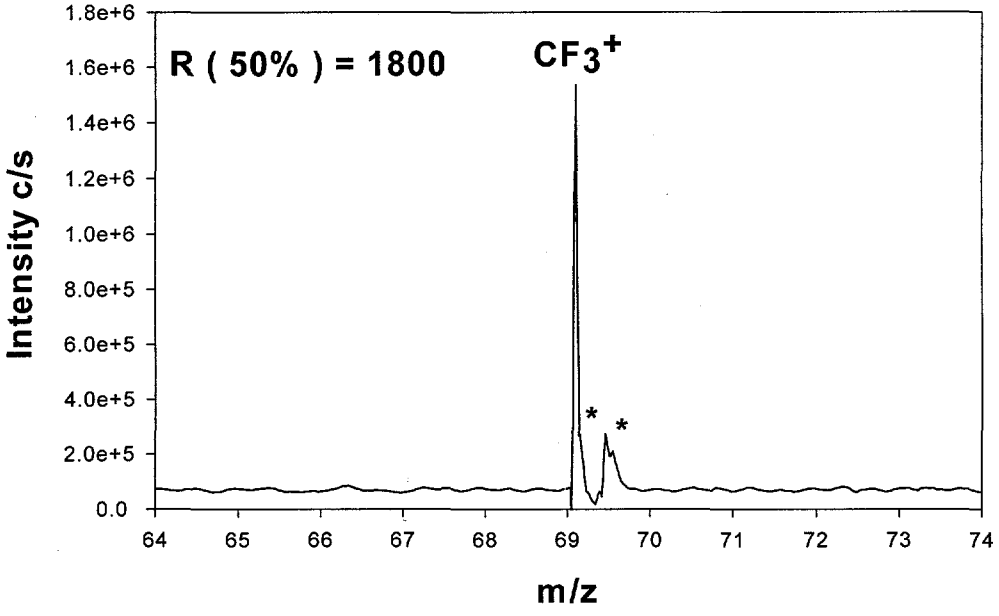

b)

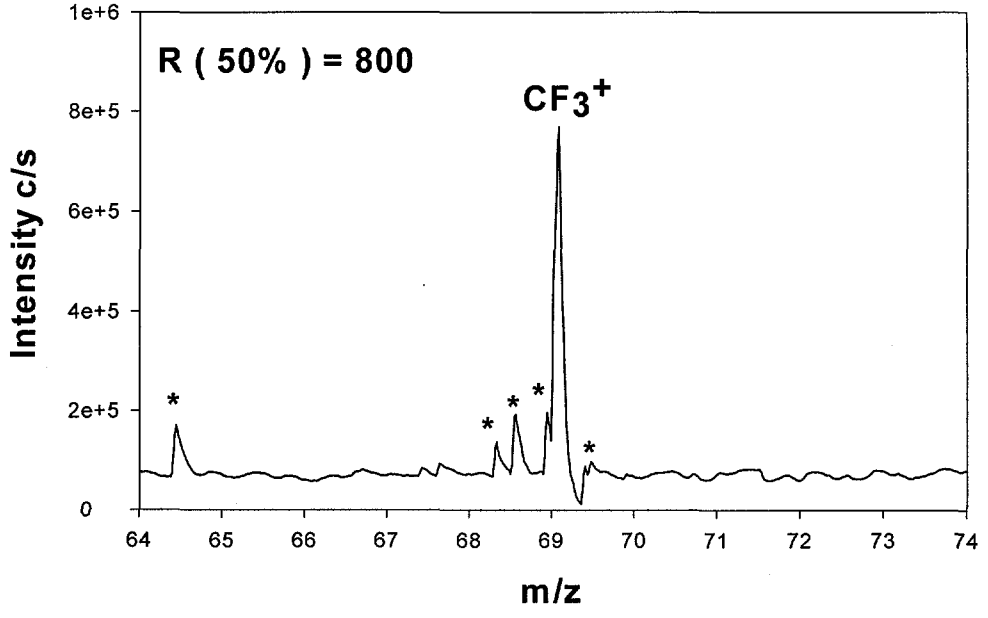

Figure 8. Scans of CF_3^+ (m/z = 69) at high resolution with the presence of artifact peaks"*" with gated ion extraction.

CHAPTER 5. FUTURE WORK AND CONCLUSION

Chapter 2 shows that inducing a mild secondary discharge between the plasma and the sampling orifice improves detection limits of the ICP-MD by increasing line intensities in the Mach disk without increasing the noise on the background. Additional improvements in detection limits could therefore be possible if the intensities could be boosted further. Future work would deal in finding ways to excite the weak analyte emission from the Mach disk while keeping the spectral background emission low. One possible way is the usage of a dye laser to populate the highly excited levels of the analyte ion. One of the problems of using a dye laser is that we will lose the simultaneous multielement capability of the echelle spectrometer.

Another way to excite the weak analyte emission while maintaining the simultaneous multielemental capability of the echelle spectrometer is to use a vacuum ultraviolet laser system. This laser should be able to populate highly excited levels of a variety of ions at the same time. These excited ions will decay to lower levels, which will decay with emission. It should be noted that the emitted UV photons can get through the quartz walls of the chamber meanwhile the laser photons will not.

Chapter 3 successfully showed that reflecting the ions inside the quadrupole mass analyzer does indeed improve the resolution. In Chapter 3 we showed that by applying a reflecting square wave voltage to the lenses at the entrance and exit of the quadrupole, the resolution improves to at least 5000. The transmission decreases as resolution improves to a similar extent as that found using quadrupoles in alternate stability regions. Using the open

circular aperture to reflect the ions multiple passes inside the quadrupole, many of the spectra had a plateau on the low mass side of the high resolution peak. This plateau is believed to be by ions that escape after one pass. To remove these stray ions, the open reflectron apertures were replaced with grids. Most of the plateau in front of the high resolution peak was removed and a resolution improved to 5000 (50 % valley). Some satellite peaks were evident in the high resolution spectra. These satellite peaks tend to be severe when the sample is a mixture of ions close in mass rather than a simple component.

To determine the basic causes of the satellite peaks and to improve the ion transmission experiments were done by storing ions from the source while shutting the beam off so that no new ions are injected while one packet of ions is reflected. Chapter 4 studies the effect of pulsing and gating the source so that a finite, non-continuous batch of ions is extracted and then reflected in the quadrupole. At the same time the pulsed ion source operates as an ion storage device. A resolution of 22,000 with 63% of the original signal remaining was obtained in this trapping-reflecting mode. In addition less stray peaks were obtained in this mode.

Experiments on demonstrating the basic concept of improving the resolution of the quadrupole mass analyzer were performed on existing ion optics supplied with the Finnigan MAT TSQ 4500 mass analyzer. These ion optics were designed for transmitting ions once not for reflecting them. Future work on improving the resolution and sensitivity by improving the ion optics arrangements. Figure 1 shows two proposed designs. In addition future work using ion optic simulation program SIMION 7.0 to model the entire multiple pass process is suggested. In addition it appears that our resolution is limited by the inherent

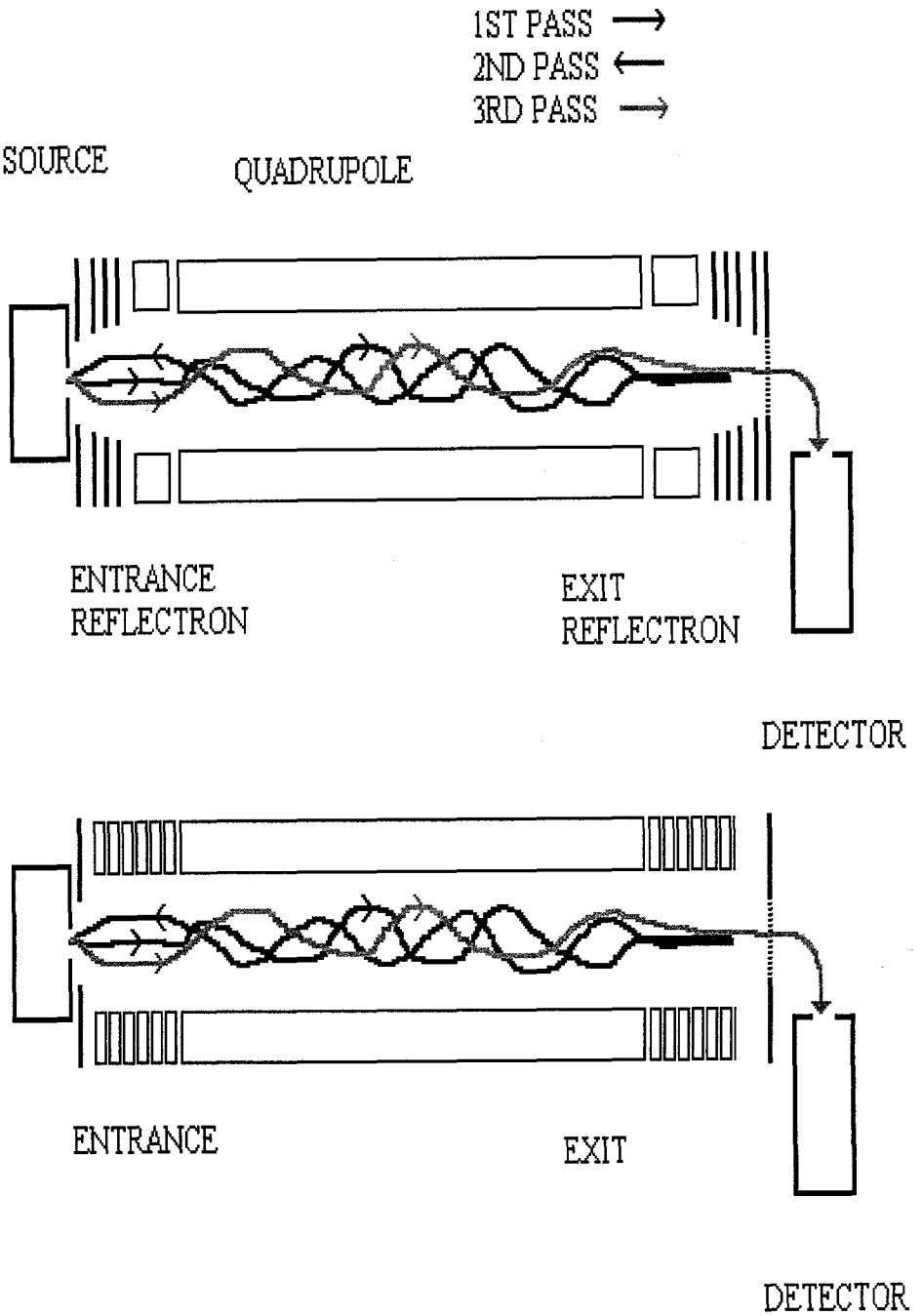

Figure 1. Suggested arrangement for reflecting ions.

peak shape of the quadrupole used. Generally, the peak shape from a quadrupole is determined by the mechanical alignment and the straightness of the rods. Different sets of quadrupoles are to be used with the segmented rf-reflectron ion optics.

Finally initial experiments were performed to improve the resolution of ICP quadrupole based mass analyzer. A resolution of 1440 was obtained at m/z 79. More work is needed to resolve the problem of polyatomic ion interferences in a quadrupole bases instrument operating at the first stability region.

ACKNOWLEDGMENTS

I would first like express my sincere appreciation and thanks to my major professor Dr. R. S. Houk for his guidance, support, tolerance and enthusiasm during my stay at Iowa State University, which made this work possible.

Sincere thanks is also extended to Dr. Marc Porter, Dr. Patricia Thiel, Dr. Keith Woo and Dr. Cheuk-Yiu Ng, who serve as a committee members. Their critical reading of this manuscript, interest and suggestions are greatly appreciated. Of course, I owe the members of the Houk group deep appreciation not only for there help in scientific discussions, but for the friendship they have shown me during my stay at Iowa State University. I especially want thank Narong Praphairasksit, David Aeschliman, Steve Johnson, Sahana Mollah, Tawhid Hasan , Zhidang Du, Jay leach, Lloyd Allen , Scott Clemons, Shen Luan, Mike Minnich and Al Gwizdala. l would like thank the chemistry machine shop , Ames lab shop , Electronics services and Dr. David Ackels. Their skills and knowledge helped me a lot.

Thanks go to all my friends who have made the years in graduate school bearable and enjoyable. Specially, I wish to thank Aref Al-Farra and Rachel Graaf for the great friendship. Special thanks for Nattash Popovic and Matthew Johll from the Johnson group. There support and long month of study made it easy to endure the long nights of pre line preparation.

This work was performed at Ames Laboratory under Contract NO. W-7405-Eng-82 with the U.S. Department of Energy. The United States government has assigned the DOE Report number IS-T 1888 to this theses.

Finally and most importantly, I would like to thank my parents Hazem Amad and Fatmeh Amad, my sisters Mai and Hannan and my brother Moiz for all their support during all the years of my education.